

**Deutsches Zentrum  
für Luft- und Raumfahrt e.V.**

**Mitteilung 2008-01**

**Particles and Cirrus Clouds (PAZI-2)**

Final Report (2004-2007)

Bernd Kärcher (ed.)

Institut für Physik der Atmosphäre  
Oberpfaffenhofen

48 Seiten  
26 Bilder  
1 Tabelle  
66 Literaturstellen



*Aerosole, Zirruswolken, Kondensstreifen, Russentstehung, Brennkammer, Klimawirkung*

Bernd KÄRCHER (Ed.)

Institut für Physik der Atmosphäre des DLR, Oberpfaffenhofen

**Partikel und Zirren (PAZI-2) – Endbericht (2004-2007)**

*DLR-Mitteilung 2008-01, 2008, 48 Seiten, 26 Bilder, 1 Tabelle, 66 Literaturstellen*

Unter Federführung des DLR Instituts für Physik der Atmosphäre untersuchten weitere DLR Institute in Stuttgart und Köln in Kooperation mit Partnern in der Helmholtz-Gemeinschaft (HGF), Universitäten und der Industrie Effekte der Russenmissionen und der von Flugzeugen generierten Kondensstreifen auf das Klima. Die komplexen Fragestellungen wurden zum einen mit Labor- und flugzeug-getragenen Messungen und Untersuchungen am DLR Hochdruckbrennkammerprüfstand HBK-S angegangen. Zum anderen kamen aufwendige numerische Simulationen von der Modellierung der Russentstehung bei Verbrennungsprozessen mit dem DLR-THETA Code bis hin zur Klimamodellierung mit dem globalen Zirkulationsmodell ECHAM4/DLR zum Einsatz.

Die vorliegende Mitteilung ruft die Projektstruktur und die wichtigsten Meilensteine in Erinnerung und fasst die wichtigsten Ergebnisse des Projektes bewertend zusammen. Neue im Projekt angestoßene Entwicklungen werden skizziert. Eine Literaturliste vervollständigt die internationale Sichtbarkeit der Projektleistungen im Bereich der Atmosphärenwissenschaften und der Russforschung.

*Aerosols, cirrus clouds, contrails, soot formation, combustion, climate impact*

*(Published in English)*

Bernd KÄRCHER (ed.)

DLR Institute for Atmospheric Physics, Oberpfaffenhofen

**Particles and Cirrus Clouds (PAZI-2) – Final Report (2004-2007)**

*DLR-Mitteilung 2008-01, 2008, 48 pages, 26 figs., 1 tab., 66 refs.*

Led by the DLR Institute for Atmospheric Physics, several DLR institutes in Stuttgart and Cologne studied effects of aircraft soot emissions and aviation-induced contrails on climate in concert with partners from the Helmholtz Society (HGF) and from universities and industry. The complex issues have been tackled on the one hand with laboratory and aircraft-based measurements as well as investigations using the high pressure combustion test rig (HBK-S). On the other hand, the formation of soot from fuel combustion and the evolution of climate have been studied by means of comprehensive numerical simulations using the DLR-Theta and ECHAM4/DLR codes, respectively.

The present report recalls the structure and major milestones and summarizes and assesses the main results of the project. New developments emerging from the project work are outlined. A list of references demonstrates the international visibility of the project in the atmospheric and soot-related research communities.

# Particles and Cirrus Clouds (PAZI-2)

DLR / HGF project (2004-2007)

Final Report



December 2007

Cover picture:

Meteosat Second Generation (MSG) Spinning Enhanced Visible and Infra-Red Imager (SEVIRI) geostationary satellite observation of a regional-scale contrail cirrus cluster and, possibly, aircraft soot-induced cirrus over Spain. The false color picture has been taken on May 28, 2004. The MSG-SEVIRI radiometer has a repetition rate of 15 min and an approximate horizontal resolution of  $3 \times 4 \text{ km}^2$  per pixel. Red and green is composed by the visible ( $0.6 \text{ }\mu\text{m}$ ) and near infrared ( $0.8 \text{ }\mu\text{m}$ ) channels, blue results from the thermal infrared at ( $10.8 \text{ }\mu\text{m}$ ). Similar scenes are seen at times in satellite observations. Figure courtesy of Hermann Mannstein, DLR-IPA.

## Foreword

Known as an active research area since the 1970s, when concerns were raised about the impact of a fleet of supersonic aircraft on stratospheric ozone, aviation-induced climate change is becoming an internationally recognized issue also within political bodies representing aviation industry and governments. Groups such as ICAO/CAEP or FAA urgently seek professional advice on how the existing state of scientific knowledge and practical applications on climate impacts of aviation may be used to inform policy decisions. Among all impacts of aircraft operations in the atmosphere, the impact on high cloudiness through the formation of contrail cirrus and soot-induced modifications of cirrus clouds is the most uncertain component and is debated most controversially.

In its second funding phase 2004-2007, the DLR-project PAZI-2 studied the interactions between aerosol particles, in particular soot emissions from aircraft jet engines, radiation and cirrus clouds in view of a possible influence of aviation on cloudiness and climate. Because of this focus, PAZI-2 supported DLR to extend its lead in the international scientific community within this area of research. The high standard of atmospheric research carried out at the DLR Institute for Atmospheric Physics (IPA), to which PAZI-2 has significantly contributed, has recently been confirmed by a panel of experts.

Under the lead of IPA, PAZI-2 has been carried out jointly with DLR-institutes in Stuttgart and Cologne, the Helmholtz Research Center Karlsruhe, and several national and international partners. Research issues focussing on contrail and soot effects on cirrus clouds and climate have been tackled with laboratory and airborne measurements at the Stuttgart high pressure combustion chamber test rig HBK-S, with the DLR-FALCON aircraft, a suite of model activities ranging from combustion models simulating soot formation with the DLR-THETA code to global models assessing climatic effects with the ECHAM code, and with remote sensing from space.

The main results of PAZI-2 are summarized and assessed in this final report. A summary of the findings from the first project phase (PAZI-1, 2000-2003) is available as a DLR Report (DLR FB 2003-18). The presentation here is guided by scientific themes rather than by the formal project structure reflecting the work packages. A list of publications that evolved from PAZI-2 is provided in the Appendix. More results will be published throughout 2008. Furthermore, annual interim project reports are available that summarize the progress made by each individual working group. This supplementary material is available via the internet.

Special thanks go to our external partners for their interest in this topic and for sharing results. I would like to mention the Aerosol Group at Karlsruhe in particular because of their dedicated contributions within the project that enabled a fruitful cooperation with IPA. This cooperation has been carried over to the Helmholtz-Society (HGF) Virtual Institute "Aerosol-Cloud-Interaction" led by FZK.

## Editor and project PI

Prof. Dr. Bernd Kärcher  
DLR Oberpfaffenhofen  
Institut für Physik der Atmosphäre  
D-82234 Weßling

[bernd.kaercher@dlr.de](mailto:bernd.kaercher@dlr.de)

Oberpfaffenhofen, December 2007



## Table of contents

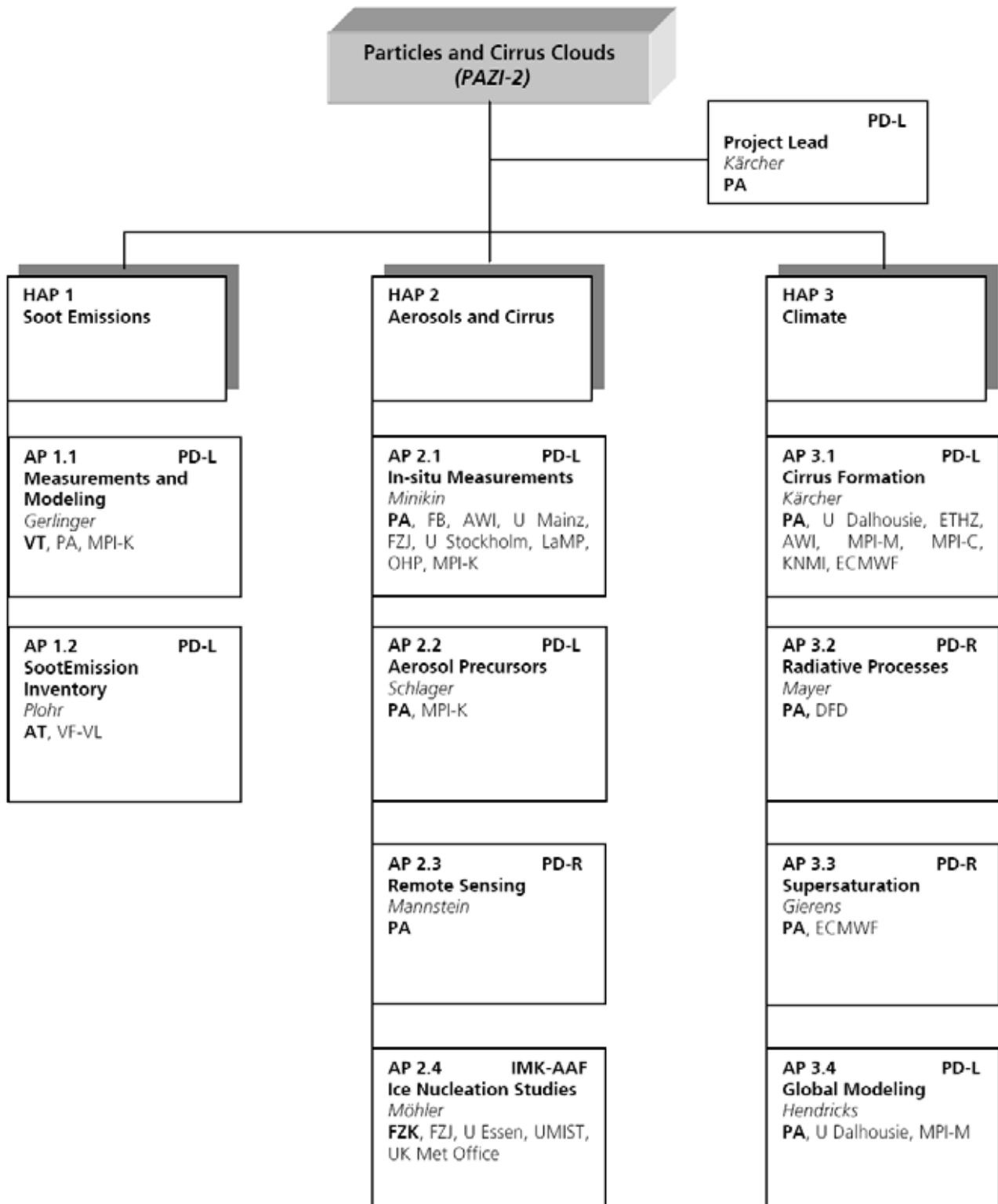
1	Structure and organization of the project .....	7
1.1	Work packages .....	7
1.2	Major goals .....	8
2	Discussion of achievements .....	11
2.1	General remarks .....	11
2.2	Project highlights and assessment of results.....	12
	First 3D simulations of the PAZI-2 combustor.....	12
	Measurements at real engines quantify particle properties at emission .....	13
	Soot oxidation reactor available for validation of detailed soot models .....	13
	First HBK-S experiments at the PAZI-2 combustion chamber .....	13
	Lightning contribution to NO <sub>x</sub> budget determined more accurately .....	15
	Trapping unifies field data of HNO <sub>3</sub> uptake in cirrus clouds .....	16
	Measuring particles in aircraft exhaust: Towards harmonizing applied methods .....	17
	ECHAM climate model coupled to comprehensive aerosol module MADE.....	18
	More accurate SO <sub>2</sub> and black carbon data available for model evaluation .....	18
	Comprehensive cirrus study sheds new light on aerosol-induced cirrus changes .....	19
	Large uncertainty in soot-induced cirrus changes .....	20
	Climate model explores possible range of effects of soot emissions on cirrus .....	21
	Climate model parameterization allows effects of IN on cirrus clouds to be studied.....	22
	Disparate water uptake explains poor partitioning of organics into ice phase .....	24
	Numerical weather prediction at ECMWF includes ice supersaturation .....	24
	MOZAIC data analyzed in search of total water and temperature fluctuations .....	24
	CIRCLE-1: Distinguishing cirrus and contrail optical and microphysical properties .....	25
	CIRCLE-2: A joint DLR/CNES cirrus cloud field campaign .....	25
	Low efficacy of contrails in forcing surface temperature .....	26
	Updated estimates of radiative forcing of line shaped contrails .....	26
	Contrail avoidance: A possible option to mitigate aviation climate impact.....	27
	Shifting of flight levels potentially reduces contrail radiative forcing .....	27
	Remote sensing reveals regional aviation impact on cirrus cloudiness.....	29
	New remote sensing data on coverage by linear contrails .....	29
	Climate model realizes contrail cirrus as an independent cloud type.....	30
	Towards global estimates of contrail cirrus coverage.....	31
	Processes controlling cirrus clouds and the contrail-to-cirrus transition .....	31
	Reduction of Cryoplane climate impact quantified.....	32
	Enhancing aviation-induced cloud cover: Aerodynamic contrails .....	33
	Heterogeneous chemistry in aircraft plumes–high sensitivity on local meteorology .....	34
2.3	Overall summary .....	34
	Soot effects and ice microphysics .....	34
	Trace gas measurements and instrument development.....	34
	Ice supersaturation and modeling of cirrus clouds.....	35
	Contrail cirrus, remote sensing and radiative transfer.....	35
2.4	New developments initiated by PAZI-2.....	35
	New condensed soot production mechanism and nano-soot generator available .....	35
	New HGF Junior Research Group AEROTROP focussing on aircraft-induced O <sub>3</sub> -changes .....	36
	New statistical cloud scheme for ECHAM5 .....	36
	New fast assessment tool to evaluate aviation climate impact.....	37
Appendix:	List of research publications (as of December 2007).....	39



# 1 Structure and organization of the project

## 1.1 Work packages

Major work packages (HAP), work packages (AP) and their leads, associated project partners and programmatic responsibility of the project are summarized in the chart below:



## 1.2 Major goals

Major milestones (HMS) of the project have been defined as follows:

HMS 1	Soot oxidation measurements completed and existing models describing soot formation improved and validated	December 2006
HMS 2	4D soot emission inventory available	June 2007
HMS 3	Measurement campaigns (HBK-S and jet engines) performed and 3D simulations incl. soot formation validated	December 2007
HMS 4	Airborne campaign CIRCLE-1 completed and ice nucleation properties of aerosol particles determined	October 2005
HMS 5	Airborne campaign CIRCLE-2 completed, climatically important parameters of cirrus determined and remote sensing methods validated	October 2006
HMS 6	First estimate of the indirect effect of soot from aviation sources on cirrus clouds	December 2007
HMS 7	Aerosol-Cirrus module in ECHAM implemented and validated	December 2005
HMS 8	Ice nucleation parameterization including homogeneous and heterogeneous processes ready for use in ECHAM	June 2006
HMS 9	Aircraft-induced changes in cloudiness and associated climate change quantified	December 2007

HMS 1: A new soot oxidation reactor has been constructed and a large number of soot oxidation experiments have been performed. Additionally a second reactor with an improved design (several side branches) is used in 2008 because the results obtained in PAZI-2 have been very promising. Large sets of experimental data concerning different parameters influencing soot oxidation are now available. These data are used to control and improve the detailed soot model.

HMS 2: The DLR emission inventory tool has been successfully improved. New representative aircraft-engine combinations have been defined which for the first time are representative in terms of fuel flow, NO<sub>x</sub> emissions and soot emissions. Due to unforeseen difficulties of data supply, no inventory could be produced to date, but data acquisition has now successfully been finished and inventory production will start soon. To overcome these difficulties an additional tool has been created to produce waypoint data on a statistical basis, where only OAG data is available. Improving the soot correlation method on the basis of measurement data (HMS 3) was not possible up to now, because of delays of the measurements schedule. The data are now available and due to the delayed emission inventory calculation, it is still possible to include results of the improved soot correlation in the inventory process.

HMS 3: A new combustion chamber with optical access has been constructed, built and investigated at the HBK-S. Thermoacoustic oscillations occurred unexpectedly during the first tests which required additional investigations and techniques for their reduction. This caused a delay of the experiments and the modified combustor has been investigated in 2007. These investigations are completed. Several measurement campaigns using real combustors or engines have been performed and analyzed. They include measurements behind small planes

(Robin and Piper), Citation Jets from the Swiss Air Force, a Rolls-Royce Combustor and a Turbomeca helicopter engine. The development, investigation and validation of a new soot model and PDF (probability density function) approach for simulations of aeroengine combustors has been completed as planned. Due to the complexity of chemistry and fluid flow in real engines this work has to be carried on to achieve more reliable 3D predictions.

HMS 4: The CIRCLE-1 campaign was carried out with a changed focus. CIRCLE-1 was organized by the PAZI-2 team at DLR-IPA jointly with the LAUNCH experiment carried out by the German Weather Service (DWD). Measurements of contrails and relative humidity have been performed. The team gained significant experience in the current ability to forecast contrail occurrence and persistence, important for air traffic management operations aiming at contrail mitigation. In addition, ice nucleation measurements involving a variety of soot particles have been carried out in the Karlsruhe aerosol chamber AIDA by the external project partner IMK-AAF.

HMS 5: The start of the CIRCLE-2 campaign was delayed by more than one year because of the unexpected late launch of CALIPSO (lidar in space). The campaign has been successfully conducted with the French colleagues from CNRS and data are currently being analyzed (first science meeting December 4/5, 2007). Based on data screenings, we expect to make headway in characterizing cirrus with remote sensing methods. In-depth analyses and preparation of research articles in concert with CNRS and the University of Mainz are planned for 2008.

HMS 6: Based on preliminary parameterizations delivered to the global modelers, a first estimate of the indirect effect of soot from aircraft engines on cirrus clouds has been performed. Cirrus modifications by aviation soot are possible but uncertain in magnitude and sign. The results are preliminary because competition between solid and liquid particles during cirrus formation was not yet included. Global simulations with a unified ice nucleation parameterization are currently being performed and these results will lead to a refinement of possible cirrus changes early 2008.

HMS 7: As a prerequisite to drive the unified ice nucleation scheme (see HMS 8), an aerosol-cirrus module has been implemented, allowing for the separate prognostic treatment of multiple ice modes originating from different aerosol sources. The modified cloud microphysical module in ECHAM has technically matured, but validation is difficult owing to a lack of data sources and is considered an ongoing process. Several research issues have been identified that need to be studied in future work.

HMS 8: A unified ice nucleation parameterization scheme including homogeneous and heterogeneous processes has been designed and completed as planned. More work than estimated was necessary to implement that scheme into the ECHAM climate model. The model system has been thoroughly tested and produces stable results (see HMS 6).

HMS 9: The PAZI-team decided during its mid-term meeting to alter the work plan and place additional emphasis on contrail climate impact. It was decided to develop a radically new concept and represent contrail cirrus as an individual cloud type in ECHAM. The updated cloud scheme is able to prognose contrail coverage and ice water content consistent with the sub-grid scale formulation of relative humidity and allows the simulation of the whole life cycle of contrail cirrus for the first time. First results on contrail-induced changes in cirrus cloudiness have become available. Improvement of optical properties of contrail cirrus to simulate their radiative forcing and quantification of the associated climate change is subject to ongoing work.



## 2 Discussion of achievements

### 2.1 General remarks

The PAZI-2 webpage <http://www.paop.dlr.de/pazi/> contains general information on the project goals and includes links to download the original proposal, a mid-term summary report, progress report sheets for all work packages, a list of publications arisen from this project and viewgraphs prepared by the project PI summarizing the annual project meetings.

Many project results have been communicated in numerous scientific conferences and workshops. Meetings with a broader scope to which members of the PAZI-2 team provided input include:

- ETH-Conference on Combustion Generated Nanoparticles, 2004, Zurich, Switzerland.
- EGU General Assemblies, 2004-2006.
- NCAR Workshop on Ice Initiation in Clouds, 2004, Boulder, CO, U.S.A.
- SPARC Third General Assembly, 2004, Victoria, Canada.
- IGAC-NOAA-NASA Specialty Conference on Indirect Effects of Aerosols on Climate, 2005, Manchester, UK.
- AIAA Aerospace Sciences Meeting, 2005, Reno, U.S.A.
- CEAS/KATnet Conference on Key Aerodynamic Technologies, 2005, Bremen.
- 24th Annual AAAR Conference, 2005, Austin, U.S.A.
- International Conference on Transportation, Atmosphere and Climate (TAC), 2006, Oxford, UK.
- Workshop on the Impacts of Aviation on Climate Change, 2006, Boston, U.S.A.
- 25<sup>th</sup> International Congress of the Aeronautical Sciences (ICAS), 2006, Hamburg.
- ECMWF Workshop on Parametrization of Clouds in Large-Scale Models, 2006, Reading, UK.
- 7. Deutsche Klimatagung (DKT), 2006, Munich.
- AIAA/ASME/SAE/ASEE Joint Propulsion Conference & Exhibit, 2006.
- 30<sup>st</sup> International Symposium on Combustion, Chicago, 2006, U.S.A.
- AGU Fall Meeting, 2006, San Francisco, U.S.A.
- Joint CloudSat/CALIPSO Science Team Meeting, 2007, San Francisco, U.S.A.
- First CEAS European Air and Space Conference Century Perspectives, 2007, Berlin.
- ICAO/CAEP Workshop on Assessing Current Scientific Knowledge, Uncertainties and Gaps Quantifying Climate Change, Noise and Air Quality Aviation Impacts, 2007, Montreal, Canada.
- ASME Turbo Expo Conference, 2007, Montreal, Canada.

## 2.2 Project highlights and assessment of results

### First 3D simulations of the PAZI-2 combustor

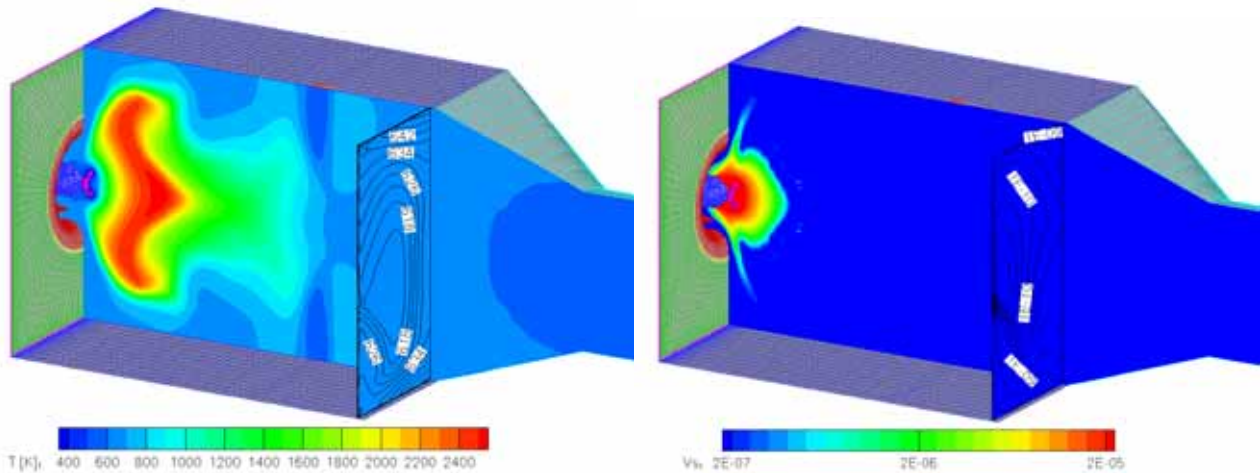


**Figure 1** Simulated distribution of temperature (left panel) and soot volume fraction (right panel) in the PAZI-2 combustor with secondary air injection.

The simulations are based on a reduced kinetic scheme for kerosene (60% n-decane, 28% iso-octane, 12% toluol) which consists out of 72 species und 150 reactions. Soot is modelled by a sectional approach for the PAHs and transport equations for soot particle number density and soot volume fraction. To take turbulence chemistry interaction into account a multi-variate assumed PDF approach is employed. Figure 1 shows calculated temperature and soot distributions. The flow is entering through a double swirler nozzle on the left side which is completely discretized. The figures show results in the symmetry and the exit plane as well as the computational grid. The simulation is performed according to an experiment with 10 bar combustor pressure. Secondary air is injected through holes in the upper and lower walls which strongly decreases the temperature and soot concentrations at the combustor exit. In the present simulation the fuel is injected in gaseous form. The results will be further analyzed and compared with the experimental data.

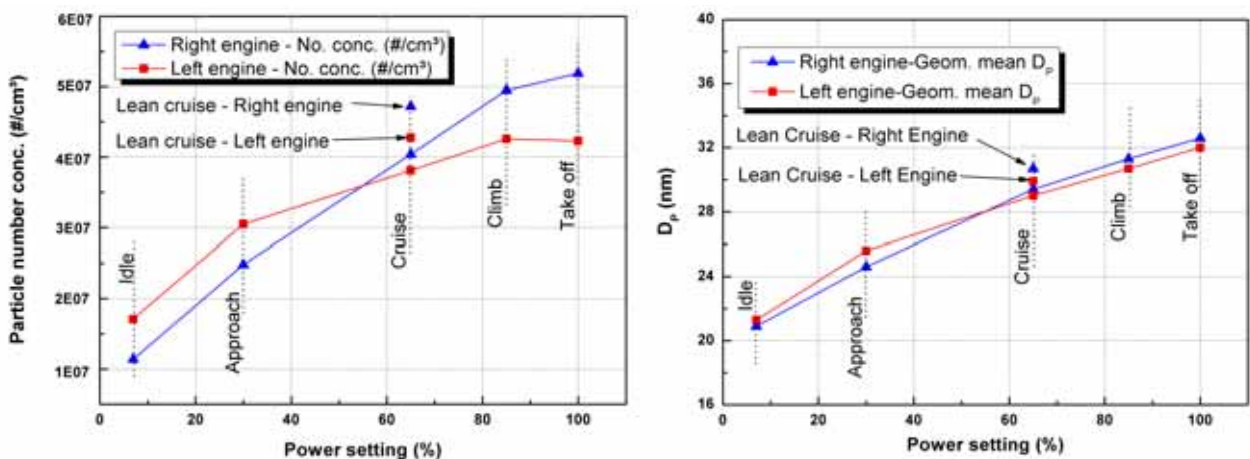


**Figure 2** Measured particle number concentrations (left panel) and mean particle diameters (right panel) for left and right engines at different power settings.

### Measurements at real engines quantify particle properties at emission

A number of campaigns have been performed by VT where the exhaust gases and particles (particle number density and size distribution) have been measured behind combustors and real engines. One such campaign employed a Cessna Citation aircraft at the airport in Bern which has been performed in cooperation with the "Bundesamt für Zivilluftfahrt der Schweiz". In this case the engine was a Pratt & Whitney PW 545 A with a bypass ratio of 3.5. Besides  $\text{CO}_2$ , CO,  $\text{NO}_x$  measurements, an EEPS is used to determine soot particle size distributions. Figure 2 shows measured particle number concentrations and mean particle diameters at different power settings.

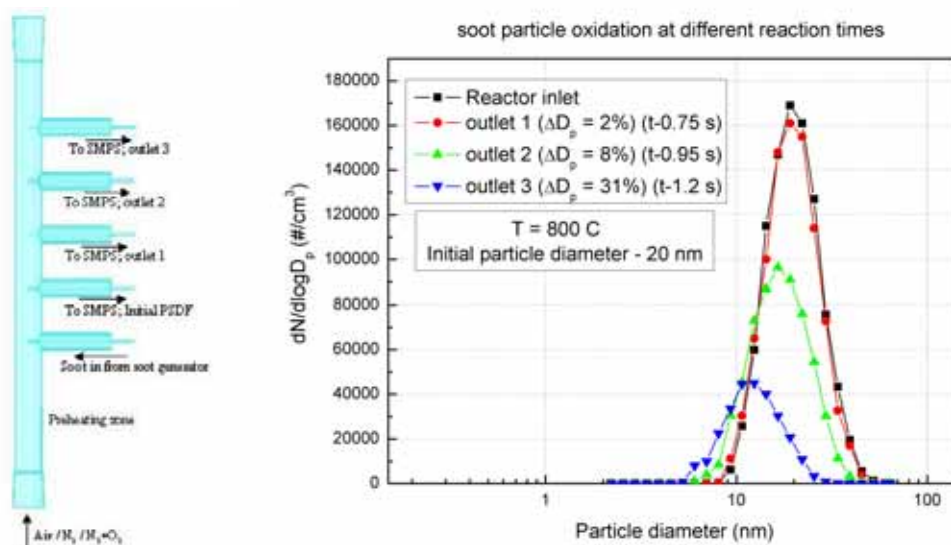


**Figure 3** Soot oxidation reactor schematic (left panel) and measured soot particle size distribution (right panel) after different times at different spatial positions.

### Soot oxidation reactor available for validation of detailed soot models

A new soot oxidation reactor has been constructed with improved a design. The new reactor with multiple side branches (see Fig. 3) offers the opportunity to perform the experiments by varying only one parameter. In the new reactor, the intermediate side branches give the chance to collect soot samples from the reactor at different reaction time points and hence without the need to change the gas flow. Soot particle oxidation experiments were conducted from room temperature till 1200 K with different reaction media and different mean particle diameters (20 nm and 28 nm). Soot oxidation was observed to start at 1000 K with a strong increase in oxidation rate with increasing temperature. Figure 3 (right panel) shows particle size distributions after different oxidation times. As expected the mean particle size and the particle number decreases with increasing oxidation time. From such experiments parameter for soot reaction rates are extracted, enabling significant progress in basic research relevant to soot emissions.

### First HBK-S experiments at the PAZI-2 combustion chamber

The newly developed PAZI-2 combustor with optical access has been investigated at the high pressure test rig HBK-S in Stuttgart. This test facility is able to reproduce conditions at the combustor inlet which agree to those of real engines. Besides probe measurements at the combustor exit, Laser measurement techniques have been used inside the combustor to obtain information on soot formation and oxidation. The combustor uses kerosene and a dou-

ble swirler nozzle at the inlet. Moreover, secondary air may be injected as in real engines in order to reduce the exit temperature and the amount of soot produced in the fuel rich reaction zones. Laser induced incandescence (LII) is used for 2D-measurements of soot volume fraction. Moreover, CARS has been used for temperature measurements at least under conditions with low soot production. Figure 4 shows measured soot volume fractions in the combustor at different pressures (10 and 5 bar). The flow is directed from left to right. Soot production strongly increases with increasing pressure. On the other hand, soot oxidation caused by secondary air injection (from top and bottom after  $\sim 2/3$  of the combustor length) is very effective and most of the soot particles are oxidized before reaching the combustor outlet.

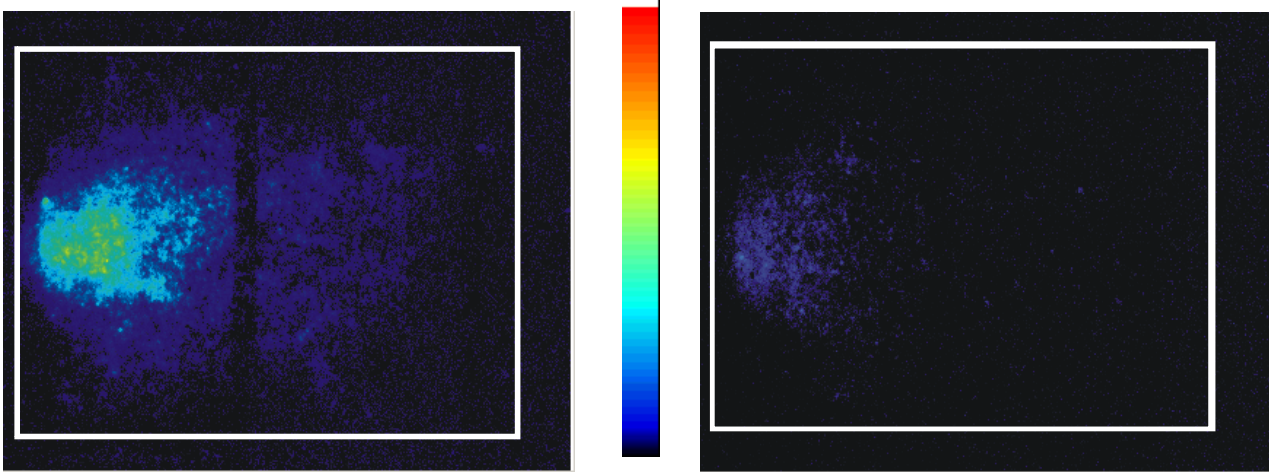


**Figure 4** Measured soot volume fractions on the PAZI-2 combustor with oxidation air ( $\phi = 1.2$ ,  $\Delta p = 2.6\%$ ). Left side  $p = 10$  bar, right side  $p = 5$  bar). Color bar indicates values in the range 0 ppm (black) to 0.1 ppm (red).

The influence of pressure, mass flow and stoichiometric ratio on soot oxidation has also been investigated. For two sets of flow conditions, temperature measurements have been performed. 1200 single shots have been performed at any single position which allowed us to investigate temperature PDF structures. Figure 5 shows statistics of these temperature measurements for two positions on the combustor axis (30 and 55 mm downstream of the injector). Especially the second distribution is far from a Gaussian which is prescribed in the assumed PDF approach of the 3D CFD simulations.

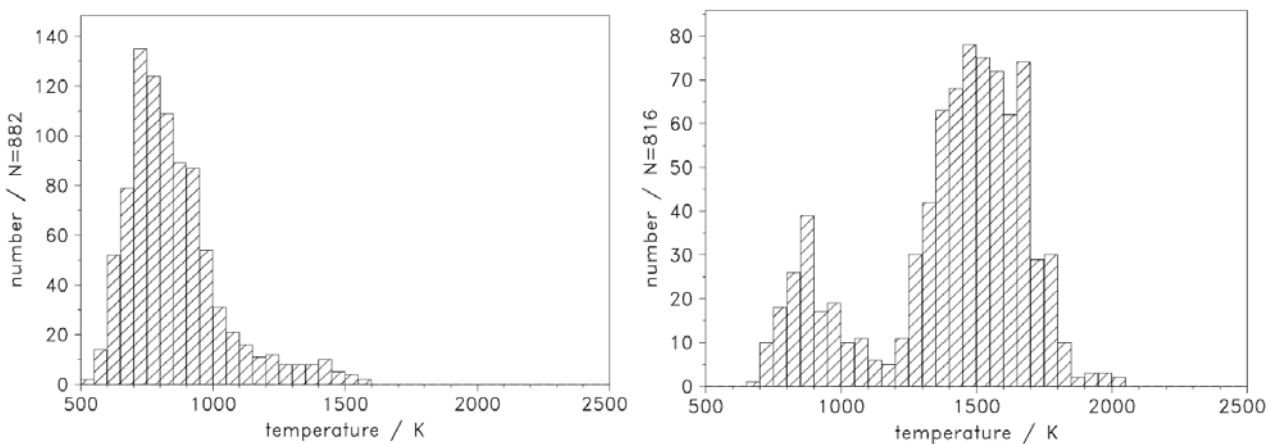


**Figure 5** Temperature PDF obtained from 1200 single shot CARS measurements at different position on the combustion chamber axis. Left panel: 30 mm, right panel: 55 mm downstream of the injector.

*Lightning contribution to NO<sub>x</sub> budget determined more accurately*

Past uncertainty in the amount and distribution of lightning-induced nitrogen oxides (LNO<sub>x</sub>) caused at least a factor-of-two uncertainty in assessing the aviation NO<sub>x</sub> impact on midlatitude ozone. LNO<sub>x</sub> is important for NO<sub>x</sub> and ozone budgets globally, since LNO<sub>x</sub> contributes ~70% (~30%) to the tropical upper troposphere NO<sub>x</sub> (O<sub>3</sub>) budget.

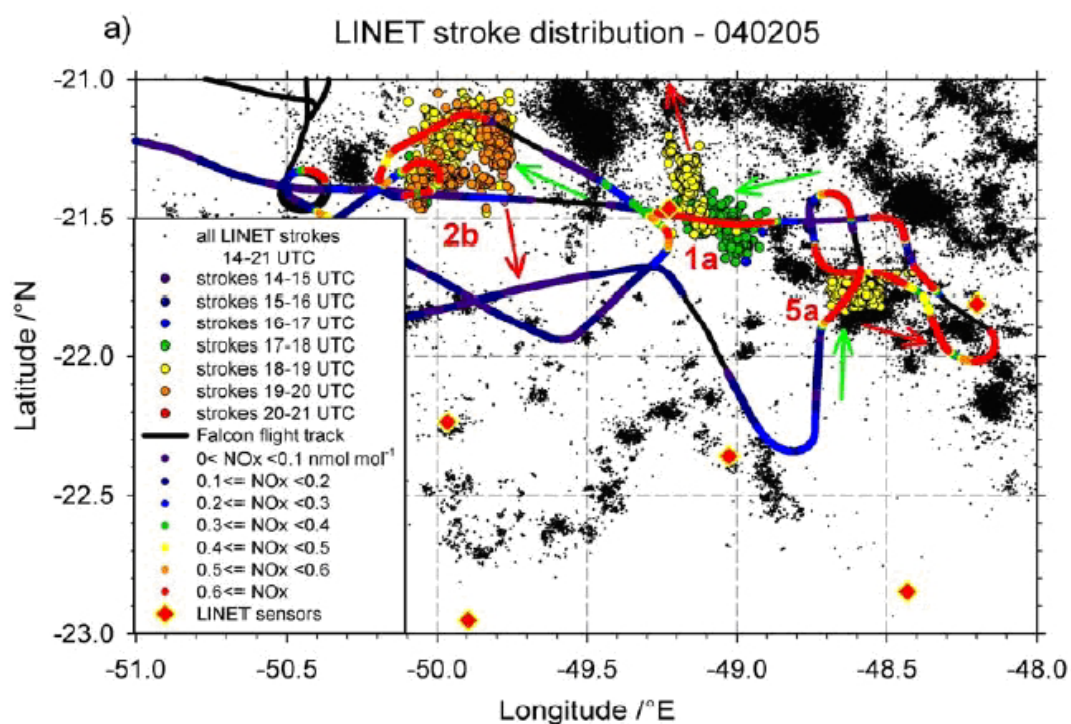


**Figure 6** Horizontal distribution of LINET strokes (4 Feb 2005) with stroke registered before the Falcon penetration indicated by colored circles. Falcon flight path is superimposed with NO<sub>x</sub> mixing ratios indicated by color scale. Red arrows indicate the storm motion direction and green arrows the wind direction. The positions of the six LINET sensors are indicated.

Measurements were performed near and inside thunderstorms over tropical continents where lightning activity is largest. Cloud-to-ground and intracloud flashes with peak currents larger than ~1 kA were located in conjunction with Radar and satellite observations with the new ground-based lightning detection system LINET (Figure 6). The related trace gas distribution (NO, NO<sub>y</sub>, O<sub>3</sub>, CO, etc.) was measured with partially new airborne instruments on the Falcon and the Geophysica at up to 20 km altitude near thunderstorms under tropical and subtropical conditions in Brazil (EU-project TROCCINOX), Australia (SCOUT-O3), and Africa (AMMA). The results were analyzed and interpreted using trajectories, and with cloud-scale and global models. An example for the latter is given in Figure 7. Moreover, previous IPA airborne measurements during the EU-project EULINOX (1998) near thunderstorms over Bavaria were analyzed with cloud-resolving models.

We found that the LNO<sub>x</sub> contribution per flash from strongly sheared subtropical and midlatitude storms, and in particular from mesoscale convective systems, is larger than from tropical cases with little vertical wind shear. From an extensive review of these and other results, a "typical" thunderstorm flash was determined to produce 250 mol NO<sub>x</sub> or 3.5 kg of N mass per flash with uncertainty factor 0.13–2.7. Multiplying the flash-specific value with the satellite-derived global flash frequency of 44 s<sup>-1</sup> gives a global LNO<sub>x</sub> nitrogen mass source rate of 0.6–13 Tg a<sup>-1</sup>. More accurate estimates may be achieved by fitting the results of high-

resolution global model variants, driven with analyzed meteorological fields, to observations. A fit of model results to TROCCINOX data provides a best-estimate LNO<sub>x</sub> source of 4.8 Tg a<sup>-1</sup> with uncertainty range 2.3–7.3 Tg a<sup>-1</sup>.

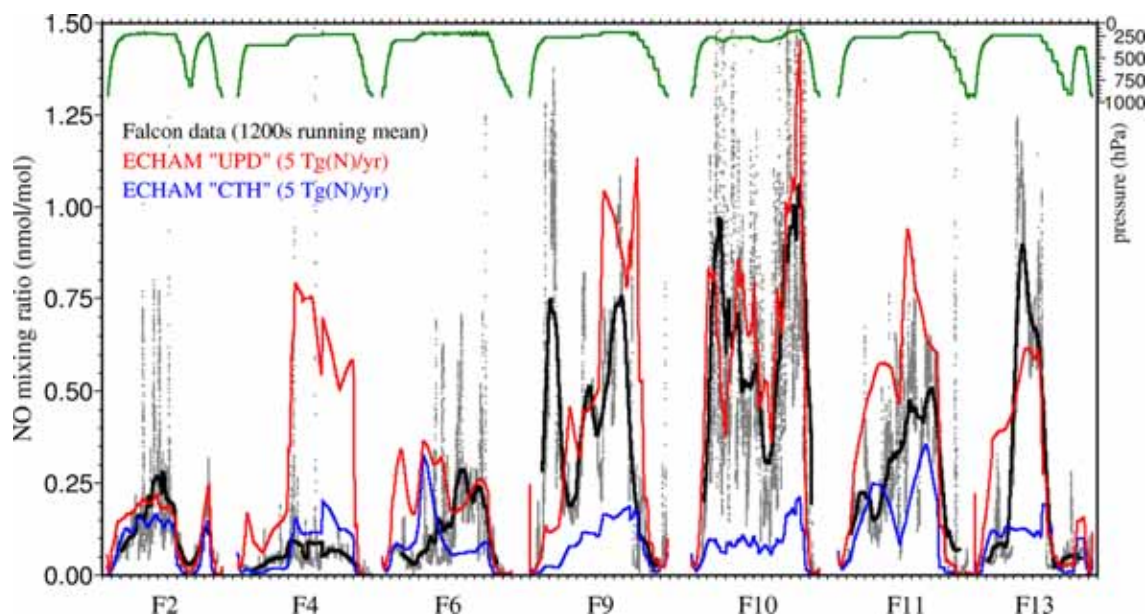


**Figure 7** Measured and modelled NO mixing ratio versus time for TROCCINOX 2004. The total measurement time during the flights F2 (14 Feb) to F13 (7 Mar) is ~30 h. Measured values (dots and line, mean value for a running average over 1200 s), and results for ECHAM with an updraft-based model (UPD, red) and cloud-top-height based model (blue, CTH), both for 5 Tg a<sup>-1</sup> LNO<sub>x</sub> nitrogen source rate.

Future research aims at quantifying the LNO<sub>x</sub> source and its distribution more accurately. The global ECHAM5/MESSy model will be improved to better represent lightning and LNO<sub>x</sub> observations; the model parameters will be used to fit the results to the growing number of trace gas and lightning observations from satellite and in-situ measurements in lightning-sensitive regions. Moreover, lightning information will be used for improved weather prediction. A lightning model will be included in COSMOS-DE. We also consider installing a lightning locating sensor on HALO. Finally, we may help EUMETSAT to include a lightning detector on the "Meteosat Third Generation".

#### *Trapping unifies field data of HNO<sub>3</sub> uptake in cirrus clouds*

A robust knowledge of cirrus cloud effects on the partitioning of NO<sub>y</sub> species is also required to quantify the effect of aviation NO<sub>x</sub> emissions on the ozone balance. Nitric acid (HNO<sub>3</sub>) in cirrus ice crystals has been measured, mostly by IPA, in the last decade during airborne campaigns at latitudes 53°S–68°N. These data have been compiled and presented as HNO<sub>3</sub>/H<sub>2</sub>O molar ratios in ice (Figure 8). The molar ratios in ice exhibit a clear upward trend with decreasing temperature and are explained by a novel model describing dissolution of HNO<sub>3</sub> in liquid aerosol particles serving as freezing nuclei and subsequent trapping of HNO<sub>3</sub> during ice crystal growth.

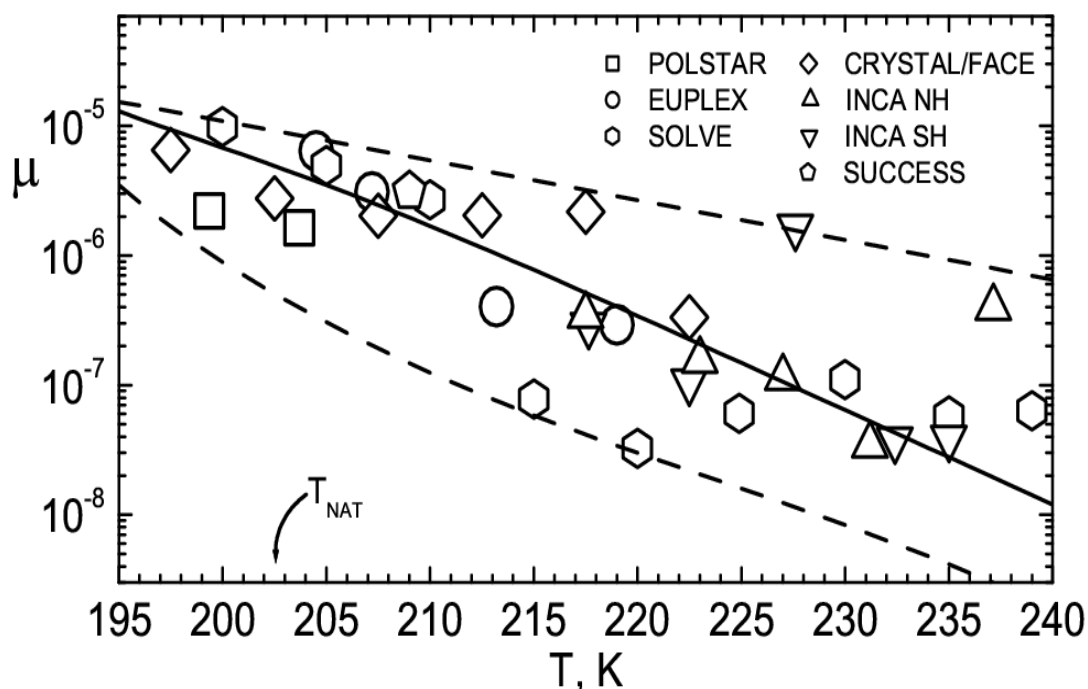


**Figure 8** HNO<sub>3</sub>/H<sub>2</sub>O molar ratios in ice versus temperature from the trapping model (solid curve) and from field data (symbols). Dashed curves represent limiting values. The efficiency of trapping increases with decreasing temperature.

The trapping model generalizes previous uptake concepts employing equilibrium adsorption isotherms by adding ice growth. This model is more adequate to describe the formation of HNO<sub>3</sub>/H<sub>2</sub>O cirrus ice particles owing to the dynamic nature of ice crystal growth. Efficient trapping occurs via diffusive co-condensation of the ambient HNO<sub>3</sub> with H<sub>2</sub>O below ~203 K, because of long residence times of HNO<sub>3</sub> molecules at the ice surface. This opens the possibility for HNO<sub>3</sub>-induced modifications of processes affecting ice growth. At warmer temperatures, molecular processes in the ice surface layer cause an increasingly rapid escape of adsorbed HNO<sub>3</sub> into the gas phase and render trapping less efficient despite faster ice growth rates.

Interpretation of data below 200 K is challenging due to unresolved issues such as the cause of persistent in-cloud supersaturation, or the presence of nitric acid trihydrate particles. Some data sets suggest high pressure saturation effects for HNO<sub>3</sub>, which should be included in future work. A final goal will be the development of a simple new parameterization of HNO<sub>3</sub> uptake for use in global chemical models.

#### *Measuring particles in aircraft exhaust: Towards harmonizing applied methods*

On request of ICAO and EASA, the SAE International Committee E-31 on Aircraft Exhaust Emissions Measurement works towards harmonized measurements used in the aeronautical industry. Recently, the key focus is on particulate matter.

A summary on methods for the measurement of non-volatile, soot-containing particles is now available as Aerospace Information Report (AIR) "Non-volatile Exhaust Particle Measurement Techniques" (SAE AIR 5892, 2004). This AIR will form the basis for an Aerospace Recommended Practice (ARP) as part of engine certification procedures. The ARPs for particle mass, particle number, and sampling are under development and will be published in the near future. The new methods will have a strong impact on the evaluation of new aircraft engines with respect to their soot particle emission characteristics. The underlying metrics are developed in collaboration with the climate research community.

### *ECHAM climate model coupled to comprehensive aerosol module MADE*

The climate model ECHAM has been coupled with the aerosol microphysics module MADE. This enables detailed simulations of the global aerosol. While previous model versions were restricted to simulations of the aerosol mass cycles, the new model system also provides information about aerosol number concentration, size distribution (in a modal approach), and particle composition. The applicability of the new model system has successfully been demonstrated by detailed comparisons with aerosol observations. Upcoming aerosol mass spectrometers such as the AMS employed by the University of Mainz during PAZI-1 will deliver more data on the chemical composition of the tropospheric aerosol in future airborne campaigns.

An model climatology of the global aerosol has been simulated, see Figure 9. The model results have been compared to the results of other global aerosol models as well as satellite data within the international AeroCom project. The latest ECHAM/MADE version includes full coupling of aerosols to a comprehensive chemistry module as well as to the climate model's radiation and cloud microphysics schemes. It is currently used to investigate the impact of ship emissions on aerosols and clouds. The model system will be applied for advanced simulations of effects of black carbon emissions on cirrus clouds.

### *More accurate SO<sub>2</sub> and black carbon data available for model evaluation*

Extended measurements of tropospheric sulfur dioxide (SO<sub>2</sub>) were performed at midlatitudes and in the tropics using the new fast-response aircraft-borne ion trap CIMS instrument. Averaged vertical SO<sub>2</sub> profiles are depicted in Figure 10 for Falcon flights performed in western Europe during INTEX-B in 2006, in southern Brazil during TROCCINOX/PAZI-2 in 2005, in northern Australia during SCOUT in 2005, and in West Africa during AMMA in 2006. Interestingly, higher median SO<sub>2</sub> mixing ratios have been observed in the free troposphere during the flights in the tropics compared with midlatitudes. Also, more variations were found for the tropical profiles as indicated by the 10 and 90% percentiles. First comparisons of the median SO<sub>2</sub> profiles with corresponding profiles from the ECHAM/MADE model have been performed, indicating significantly lower SO<sub>2</sub> mixing ratios in the free troposphere for the model profiles compared to the observations for all locations. This is a motivation to search for possible causes of this discrepancy and to ultimately improve the model.

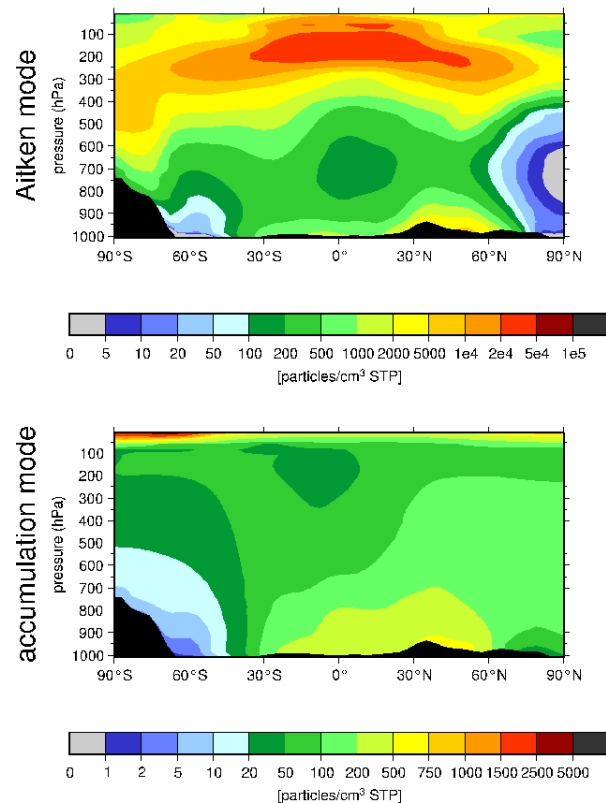


**Figure 9** Climatological annual means of simulated aerosol number concentration for Aitken (top; diameter < 0.1 μm) and accumulation mode (bottom; 0.1–1.0 μm) obtained from a 10-year integration. Shown are the zonally averaged vertical cross sections for each mode. Concentrations are given at STP.

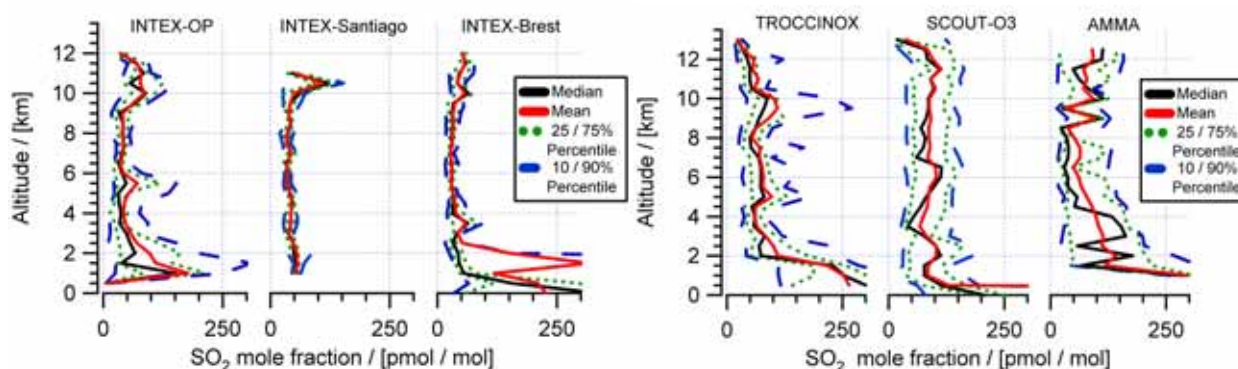


**Figure 10** Measured median and mean  $\text{SO}_2$  profiles from all flights performed out of Oberpfaffenhofen (48.1°N, 11.3°E), Brest (48.4°N, 4.4°W) and Santiago (42.9°N, 8.4°W) during INTEX (left panels) and Aracatuba (21.1°S, 50.4°W), Darwin (12.4°S, 130.9°E) and Ouagadougou (12.4°S, 1.5°W) during TROCCINOX, SCOUT, and AMMA, respectively (right panels). Also given are 25%, 75% and 10%, 90% percentiles

Colleagues from NOAA ESRL performed airborne measurements of midlatitude black carbon using laser-induced incandescence to quantify the BC mass in single aerosol particles with sizes  $> 0.15 \mu\text{m}$ . Vertical profiles of BC mass taken over Houston, TX, are shown in Figure 11 with ECHAM/MADE simulations.

While the agreement between ECHAM and observations are relatively poor in the lower stratosphere, the model compares very favourably in the troposphere, especially in regions near the tropopause, where air traffic maximizes. This result is promising and builds confidence in the proper treatment of black carbon sources (including aviation) and sinks in ECHAM to study soot effects on cirrus formation, but more in-situ data are required for a substantial model evaluation.

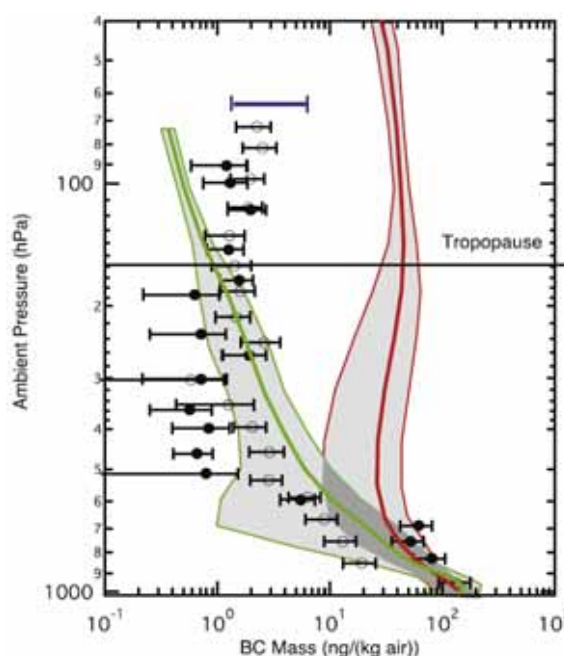


**Figure 11** Observed BC mass in single particles (symbols) versus altitude. The color curves results from the ECHAM4 (green) and LMD-INCA (red) global models. Shaded areas indicate climatological variability.

### *Comprehensive cirrus study sheds new light on aerosol-induced cirrus changes*

The APSC microphysical aerosol-cirrus model has been employed to simulate cirrus clouds along a seasonal set of ECMWF trajectories at northern midlatitudes. The model has been constrained by in-situ observations in terms of aerosol size distributions, freezing relative humidities, cooling rates, and ice particle sedimentation rates. Key features include competition between insoluble and volatile aerosol particles and temperature perturbations induced by high-frequency gravity waves unresolved by the ECMWF fields. Recent analyses at IPA of field measurements have revealed the crucial roles both factors play in cirrus formation.

We have shown that most cirrus form in synoptic cold pools, but with microphysical properties determined by small-scale variability in vertical velocities. Heterogeneous ice nuclei (IN)

present in concentrations probably typical of northern midlatitude background conditions ( $< 0.01\text{-}0.03\text{ cm}^{-3}$ ) significantly modify cirrus properties but do not control their formation. The key effect of IN is a reduction of the number of cirrus ice crystals.

This indirect aerosol effect results in reduced cirrus albedo due to increased effective radii and decreased ice water contents. Further, it causes nonlinear changes of cirrus occurrence, optical extinction (Figure 12), and sub-visible cloud fraction. The nonlinear dependence of the three latter quantities appears when IN concentrations rise well above  $\sim 0.01\text{ cm}^{-3}$ . Then, IN become the controlling factor in cirrus formation and the role of homogeneous freezing diminishes. Ice nuclei effective near ice saturation are capable of introducing strong changes of cirrus properties at low concentrations. Optically thin cirrus is particularly susceptible to IN: the presence of only  $0.001\text{ IN per cm}^3$  of air can significantly increase their occurrence frequencies. If such clouds predominantly form on such IN, they might well be affected by anthropogenic activities including aviation.

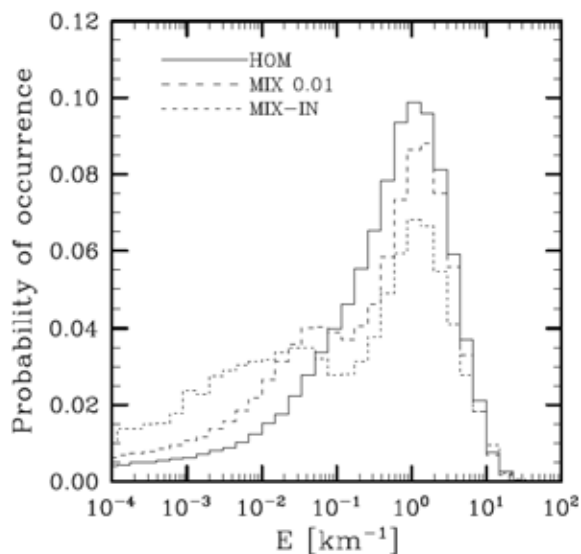


**Figure 12** Simulated probability distributions of cirrus visible extinction for homogeneous freezing only (case HOM), and with  $0.01\text{ IN per cm}^3$  of air added with ice nucleation threshold relative humidity of 130% (case MIX-0.01) or 105% (case MIX-IN).

These results provide valuable insights into cirrus modifications caused by IN. For instance, they suggest that aircraft soot-induced changes in cirrus optical properties may stay rather small unless these soot particles are very potent IN. Instead, changes in thin cloud occurrence could be more important in altering radiative forcing. However, changes in upper tropospheric cooling rates and ice-forming aerosols from sources other than aviation in a future climate may induce comparable changes in cirrus occurrence. The question of how much aircraft soot emissions contribute to cirrus changes is still open, but within PAZI-2 IPA has contributed much to enable such studies with future global model configurations (see below).

### *Large uncertainty in soot-induced cirrus changes*

While dispersing in the atmosphere, soot emissions can change the number of cirrus ice crystals, and thereby cloud radiative properties, by acting as ice nuclei (IN). The efficiency of aircraft soot to alter natural high cloudiness depends on their ice-forming ability relative to particles from other anthropogenic and natural sources, which is poorly known.

Figure 13 contains a compilation of currently available ice nucleation data for soot particles from different sources. For example, measurements carried out at FZK during PAZI-2 showed that soot particles from a spark generator (label GS) form ice very easily. However, it is questionable if this applies to jet exhaust soot at cruising altitudes. Ice nucleation behaviour appears to be strongly source-dependent.

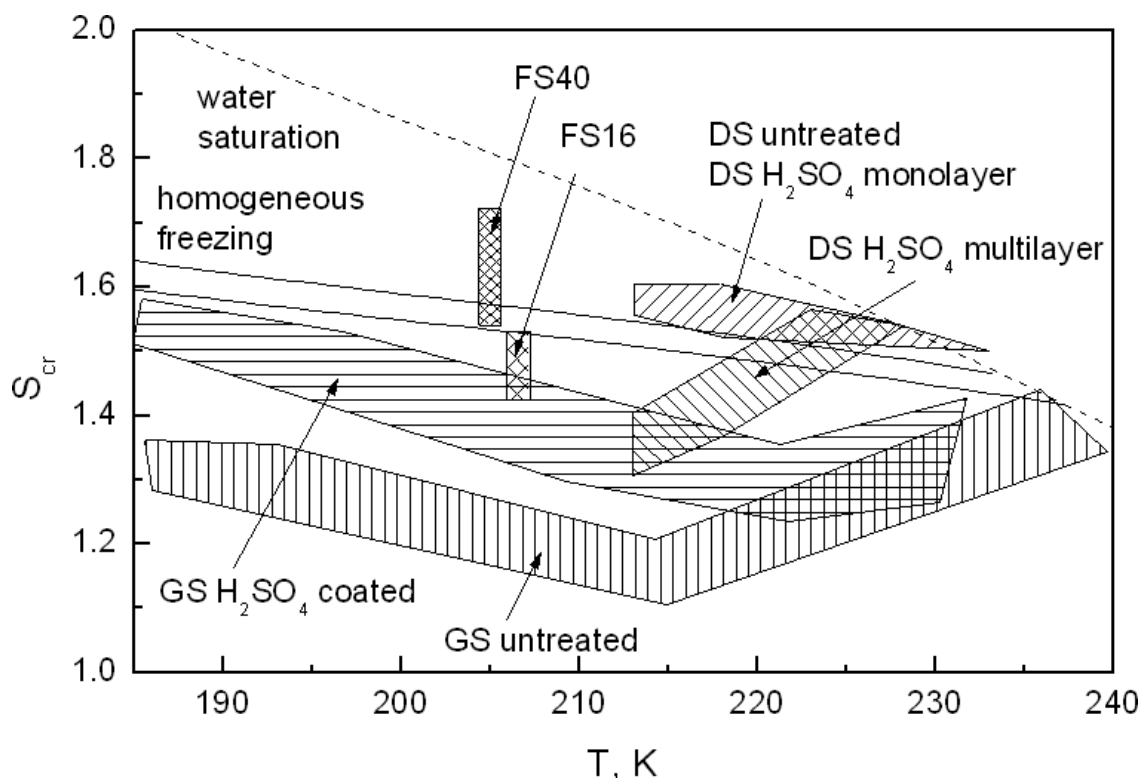


**Figure 13** Summary of threshold ice saturation ratios describing the onset of heterogeneous ice nucleation by soot particles measured in laboratory studies. Degussa soot (DS) untreated particles, and with  $\text{H}_2\text{SO}_4$  monolayer and multilayer coating; untreated and  $\text{H}_2\text{SO}_4$ -coated soot particles (GS) from a graphite spark generator; flame soot particles with 16% (FS16) and 40% (FS40) organic carbon content.

In fact, the main problem associated with assessing the role of soot-induced cirrus is our poor knowledge of the ice nucleation behavior of soot-containing particles, regardless of their source. In-situ ice nucleation measurements of jet exhaust soot particles are not available, and current laboratory evidence is inconclusive, in part because most studies employed soot samples of unknown atmospheric relevance. As a consequence, global model studies can only provide preliminary parametric studies exploring possible uncertainties of soot-induced changes in cirrus properties.

By means of IPAs comprehensive microphysical-chemical plume model developed during PAZI-2, two principal scenarios for the indirect aircraft soot effect on cirrus have been suggested: high concentrations of original soot emissions slightly increase the number of ice crystals; low concentrations of particles originating from coagulation of emitted soot with background aerosols lead to a significant reduction in ice crystal number. Ultimately, dedicated field measurements are required to unravel the soot effects and decide which of the two scenarios might actually be realized. Laboratory studies need to be continued systematically to achieve a fundamental understanding of heterogeneous ice nucleation processes and to investigate possible preactivation effects induced by short-lived contrails.

#### *Climate model explores possible range of effects of soot emissions on cirrus*

Despite current limitations to draw definite conclusions about the role of soot in atmospheric ice formation, a first explorative study has been carried out with ECHAM. Two extreme cirrus formation scenarios were considered, leading to the possible effects of soot emissions on the ice crystal number concentration (ICNC) as shown in Figure 14.

Aviation was found to cause an increase or decrease in ICNC, depending on whether cirrus formation without aviation emissions is assumed to be dominated by soot and mineral dust particles (a) or by liquid particles (b).

These scenarios demonstrate that cirrus modifications by aviation are possible. Calculated annual mean changes  $\Delta(\text{ICNC})$  caused by soot emissions are 10–60%, yielding slight changes in ice crystal sizes. The results are preliminary because competition between solid and liquid particles during cirrus formation is not yet included in the model.

*Climate model parameterization allows effects of IN on cirrus clouds to be studied*

IPA has systematically developed simple yet accurate parameterizations of cirrus formation for single nucleation modes acting in isolation. Those schemes have been implemented into the ECHAM4 climate model, resulting in a preliminary global assessment of possible effects of ice nuclei in the atmosphere, besides the aviation-related application noted above.

Recently, the full scheme has been finalized, tracking the number density and size of nucleated ice crystals as a function of vertical wind speed, temperature, ice saturation ratio, aerosol number size distributions, and preexisting cloud ice. As a major step forward, it allows for competition between heterogeneous IN and liquid aerosol particles during freezing (Figure 15).

The total number of ice crystals formed depends on the IN concentration for any given updraft speed and temperature. In the plateau regions visible in Figure 3.10, ice crystal number decreases substantially when IN are added, because IN decrease the peak supersaturation and fewer liquid droplets freeze relative to pure homogeneous freezing (gray curve). This effect is also visible in more detailed cirrus simulations and has been termed negative Twomey effect because of the apparent contrast to the traditional Twomey effect in warm clouds (adding CCN serves to increase cloud droplet number there). In-situ observations of midlatitude cirrus and satellite observations of polluted aerosol and ice cloud properties over the Indian Ocean lend support for the existence of the negative Twomey effect.

The novel scheme establishes a flexible microphysical framework for a comprehensive assessment of indirect aerosol effects on and properties of cirrus in global climate, chemistry transport, and weather forecast models. It is currently being implemented into ECHAM4 and thoroughly tested and will be employed in future aviation studies aiming at bracketing the potential soot effects on cirrus clouds.

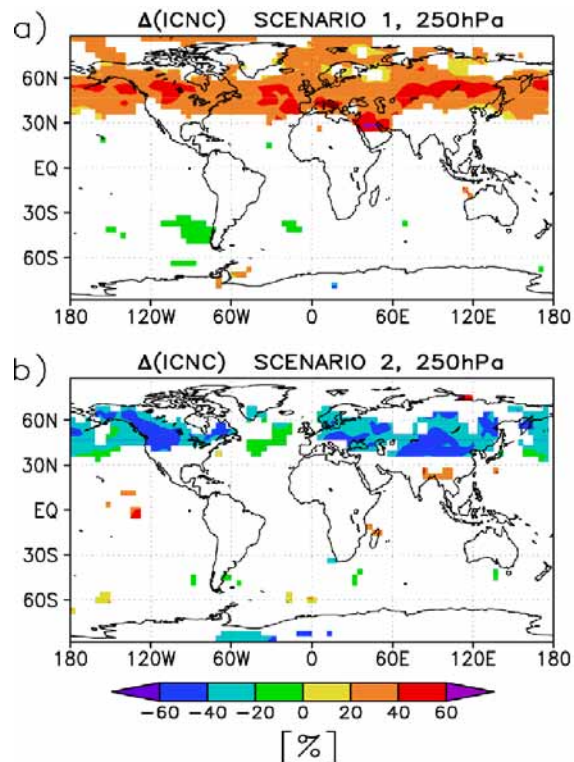


**Figure 14** Global simulations of the relative change of the annual mean ice crystal number concentration in cirrus clouds at 10 km altitude induced by soot particles from aviation. Perturbations occur in a zonal band including the main flight corridors.

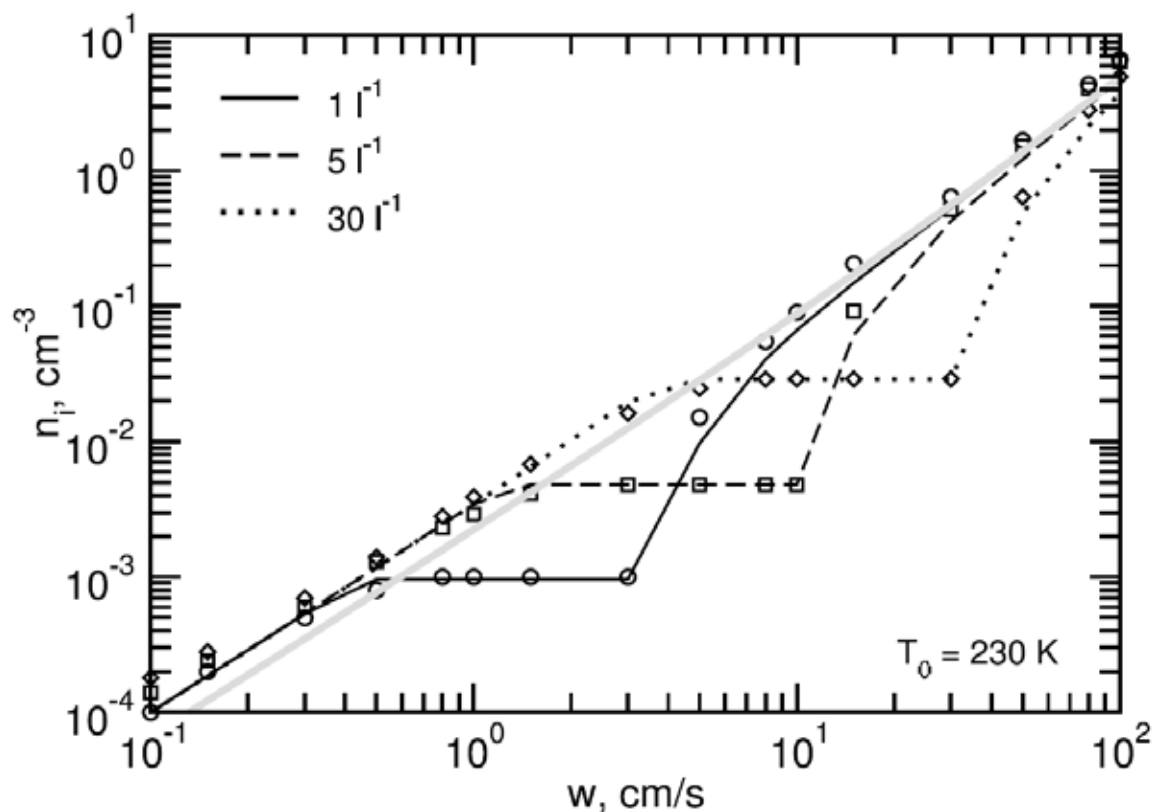


**Figure 15** Total number concentration of ice crystals formed in a cooling air parcel as a function of the vertical velocity for an initial temperature of 230 K (curves: parameterization; symbols: numerical simulations). The total number concentrations of heterogeneous ice nuclei activating ice at 130% relative humidity over ice are indicated in the legend. The thick gray curve represents pure homogeneous freezing.

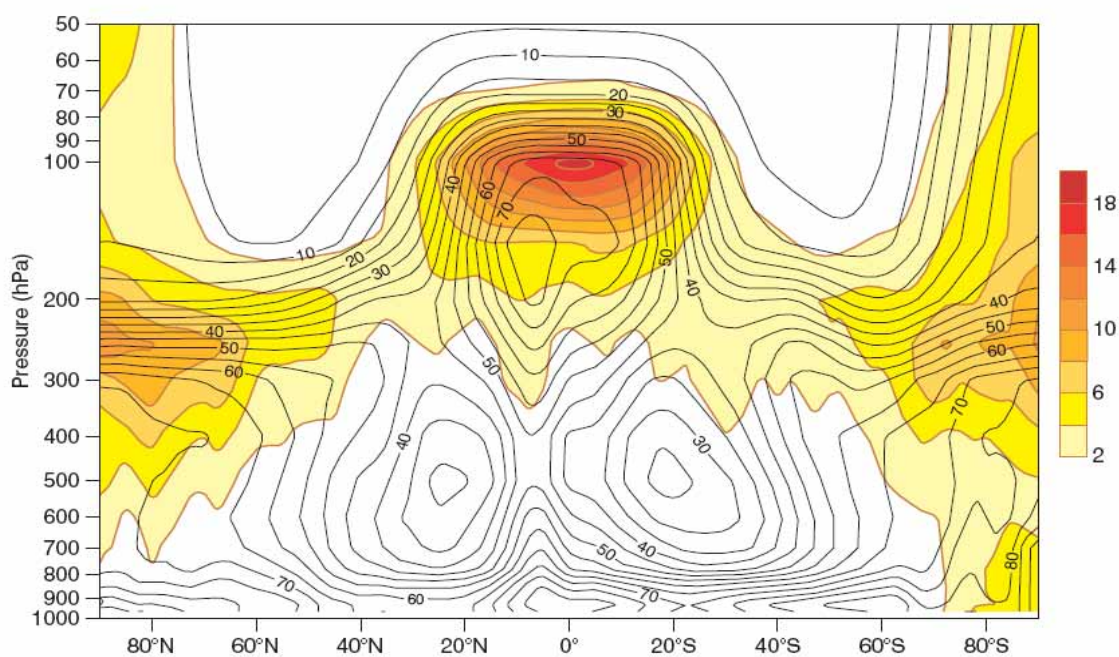


**Figure 16** Difference in zonal mean relative humidity between experiments with the ECMWF integrated forecast system using the new supersaturation scheme and the control (shaded contours), and the zonal mean relative humidity in the control forecast (line contours with 5% intervals) based on 7-member 12-month averages.

*Disparate water uptake explains poor partitioning of organics into ice phase*

Many recent measurements of ice supersaturations near the homogeneous freezing levels (above 50%) have underscored the importance of this ice formation pathway in cirrus conditions. A modeling study was conducted with the APSC model to investigate the effects of organic solutes on the homogeneous freezing behavior of liquid aerosols.

A disparate water uptake and resulting size differences that occur between organic and inorganic particles prior to freezing has been identified as the most likely reason for the poor partitioning of organic aerosols into the ice phase as observed in field measurements. The differences in water uptake can be caused by changes in the relationship between solute mass fraction and water activity of the supercooled liquid phase, by modifications of the mass accommodation coefficient for water molecules, or by a combination thereof. These findings facilitate the treatment of organic particles in the parameterization scheme for cirrus cloud formation used in the ECHAM climate model.

*Numerical weather prediction at ECMWF includes ice supersaturation*

Cirrus clouds need ice supersaturation to form and develop. Most global models do not represent supersaturated states explicitly, but use assumptions about the subgrid scale variability of water substance to describe such states. For the first time, ice supersaturation in the upper troposphere is explicitly represented in a weather prediction model, the ECMWF Integrated Forecast System, in reasonable agreement with available observations. IPA contributed substantially to this development.

The new feature has significant influence on practical applications of meteorology. Apart from an improved representation of cirrus cloudiness and upper tropospheric humidity in the ECMWF model (Figure 16), the new feature will also be useful for persistent contrail prediction. IPA will devote substantial future work to study the potential to find the best environmentally compatible routes for intercontinental flights based on this novel analysis and prediction tool.

*MOZAIC data analyzed in search of total water and temperature fluctuations*

To compute cloud formation and coverage, large-scale atmospheric models for weather or climate prediction generally need to make assumptions on the probability density function of fluctuations of total water and temperature with respect to their grid mean values. These distribution functions are rarely checked against actual fluctuation data, which are difficult to obtain experimentally.

To provide such data, IPA has used MOZAIC data from 1995-2003 to analyze the statistics of instantaneous fluctuations of temperature, relative and absolute humidity with various spatial resolutions. Probability density functions and their low order moments have been determined, as well as their seasonal and geographical variations. Bivariate distributions of joint fluctuations of temperature and relative humidity have been derived as well. Especially for upper tropospheric conditions it was shown that temperature fluctuations cannot be neglected; instead, bivariate distributions of simultaneous fluctuations of temperature and humidity have to be taken into account. These investigations provide an observational basis for the validation of statistical cloud schemes for large-scale models.

### *CIRCLE-1: Distinguishing cirrus and contrail optical and microphysical properties*

Microphysical and optical properties of linear contrails and cirrus clouds have been measured with colleagues from LaMP during the first PAZI-2 field campaign "Cirrus Cloud Experiment" (CIRCLE-1). It was performed during the international 'Lindenberg Campaign for Assessment of Humidity and Cloud Profiling Systems' (LAUNCH) organized by DWD.

For flight planning during CIRCLE-1, model forecasts available at IPA have been significantly improved. Based on ECMWF data fields, a first step was taken to develop a prediction tool for regions where contrail formation and persistence of contrails are to be expected. Enhancing the skill of regional contrail forecasts will be subject of further research at IPA.

During CIRCLE-1 measurements of the particle size distribution of interstitial non-volatile (mostly soot) particles in fresh contrails have been performed for the first time using a diffusion battery and inversion technique. It was found that the shape of the non-volatile particle size distribution agrees with previous emission measurements taking dilution into account.

**Table 1** Table of contrail and cirrus properties measured with the Falcon during the PAZI-2/CIRCLE-1 experiment in similar meteorological conditions at ~12 km altitude. Number concentration, effective ice crystal diameter, visible extinction coefficient and asymmetry factor are abbreviated by  $n$ ,  $D_{\text{eff}}$ ,  $\beta_{\text{vis}}$  and  $g$ , respectively, IWC denotes ice water content.

	age (min)	T (K)	RHI %	$n(>1\mu\text{m})$ ( $\text{cm}^{-3}$ )	$n(>3\mu\text{m})$ ( $\text{cm}^{-3}$ )	$n(>25\mu\text{m})$ ( $\text{cm}^{-3}$ )	$D_{\text{eff}}$ ( $\mu\text{m}$ )	IWC ( $\text{mg}/\text{m}^3$ )	$\beta_{\text{vis}}$ ( $\text{km}^{-1}$ )	$g$
contrail	2.5	213	118	68.3	0.2	0.004	6	0.9	0.48	0.827
contrail	17	213	121	18.3	0.9	0.021	11	1	0.29	0.787
cirrus	—	216	125	1.4	0.1	0.15	25	2	0.3	0.790

Table 1 summarizes key results obtained for young and aged linear contrails and cirrus probed during CIRCLE-1. These observations revealed that: contrails younger than ~15-20 min contain more and smaller ice crystals, and visible extinction is larger than in nearby cirrus; the ice crystal size distributions lack a large particle mode that appears in many cirrus, and ice water content of such contrails tends to be smaller by a factor 2 than for cirrus. While this helps evaluate parameterizations for optical properties, there is an apparent lack of such data for contrail cirrus.

### *CIRCLE-2: A joint DLR/CNES cirrus cloud field campaign*

Designed and carried out during May 2007 under the PAZI-2 umbrella in close cooperation with French colleagues, CIRCLE-2 aimed at an extensive characterization of optical and radiative properties of natural and anthropogenically influenced cirrus clouds at midlatitudes to ultimately improve the parameterization of these properties in mesoscale and large-scale models. Cloud-radiation interactions were studied with the German and French Falcons at the scales of the cloud system and internal cloud structure. Besides a suite of cloud probes, the RALI (combined Radar/Lidar) was employed for advanced cloud probing. CIRCLE-2 contributes to the A-train (especially CALIPSO and CloudSat) level 2 product

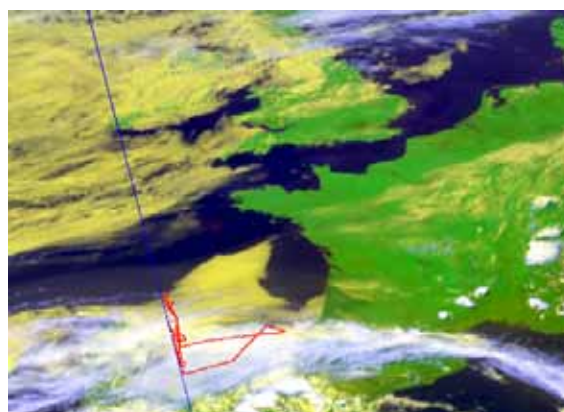


**Figure 17** MSG false color composite for 23 May 2007, at 1330 UTC. Shown are the Falcon flight path (1215–1512 UTC, red) and the coincident Calipso overpass (1338 UTC, blue).

validation, e.g., by investigating the issue of multiple scattering effects, and addresses validation of MSG cirrus retrievals developed at IPA. As an example for a coordinated measurement, the Falcon flight path between ~12:15 and 15:12 UTC (red) is shown in Figure 17 along with the coincident CALIPSO overpass track (~13:38 UTC, blue) on the MSG2-SEVIRI false color composite taken during CIRCLE-2, comprising France, the UK and Northern Spain. The latter region is covered by an extended cirrus cloud (bluish) on top of and above water clouds. This scene is particularly well suited for CALIPSO validation.

### *Low efficacy of contrails in forcing surface temperature*

Observation-based studies performed in the USA during recent years suggested a dominating impact of aviation and contrails on surface temperature trends over the USA and of a reducing contrail impact larger than 1 K on local surface diurnal temperature range. We found such claims to be unconvincing as they lack the required conceptual and statistical backing: A decadal climate sensitivity simulation involving a contrail radiative forcing of  $\sim 0.2 \text{ W/m}^2$  (artificially enhanced to mimic all aviation-induced cirrus) showed that the efficacy of contrails in forcing a surface temperature response might be smaller rather than larger in comparison to other forcing types like  $\text{CO}_2$ . The same simulation provides no evidence of any significant change in diurnal temperature range.

### *Updated estimates of radiative forcing of line shaped contrails*

The IPCC (1999) estimate of global radiative forcing (RF) caused by aircraft-induced perturbations in the year 1992 has been updated based on results from the EU-project TRADEOFF (Figure 18). The total RF from aviation for 2000 is similar to 1992, because a reduced forcing for linear contrails compensates an increase caused by increased air traffic.

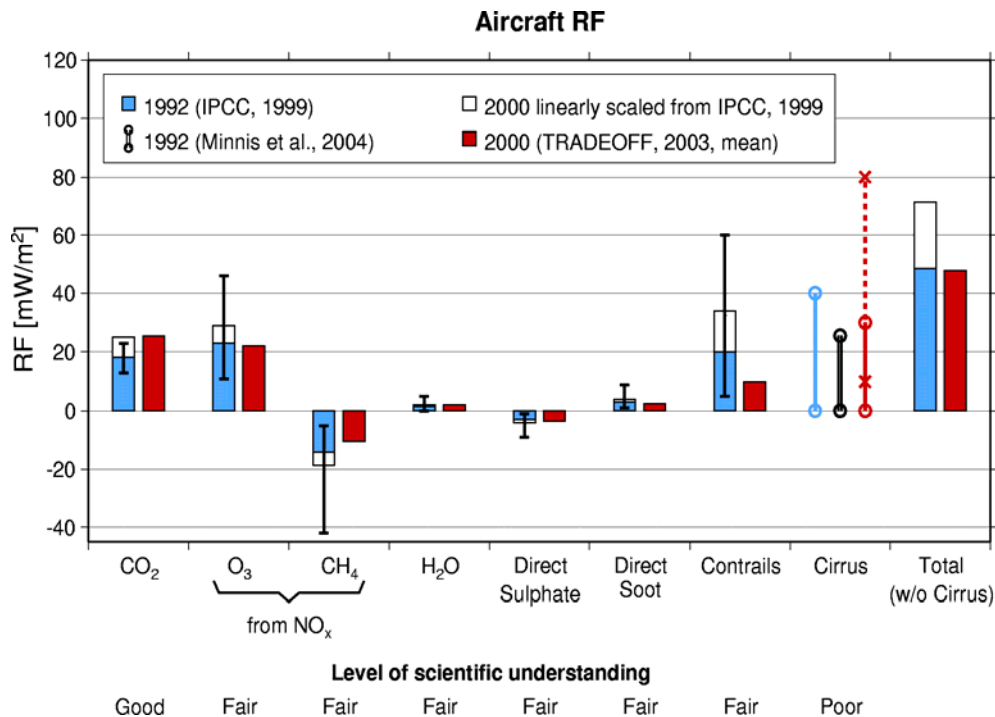


**Figure 18** Radiative forcing from aviation for 1992 and 2000 based on IPCC and TRADEOFF results. Whiskers denote 2/3 confidence intervals. The total does not include contributions from contrail cirrus and soot-induced cirrus, for which only ranges have been suggested.

The estimate of ice cloud RF is sensitive to the assumptions of optical depth, a variable that is roughly estimated from satellite data and model estimates. The downscaling of linear contrail RF is a direct consequence of the optical depth which is now estimated smaller than in IPCC (1999). This scaling is still uncertain. For example, it does only crudely account for seasonal and geographical variations.

*Contrail avoidance: A possible option to mitigate aviation climate impact*

Given a large share of contrails and contrail-induced cirrus in total aviation-induced radiative forcing, strategies are needed for avoiding contrail formation or mitigating the problem in order to reduce the impact of air traffic emissions on global warming. The ECATS network of excellence led by IPA provided a review of various strategies for contrail avoidance, covering both technical (addressing changes in engine technology) and operational (tied to air traffic management) options. A technical option includes the question whether fuel additives could be used to suppress contrails. We could show, by reanalysing a number of flight experiments using kerosene with varying sulphur content, that it is extremely difficult to affect the thermodynamically controlled contrail onset conditions with fuel additives. It was concluded that fuel additives are not a viable contrail mitigation option. However, it was noted that fuel additives might serve to change contrail optical and microphysical properties which could render them less detrimental for the climate.

*Shifting of flight levels potentially reduces contrail radiative forcing*

IPA also addressed possible operational measures to avoid persistent contrail formation. By analyzing one year of high resolution research radiosonde data over Lindenberg, Berlin, it was found that relatively small changes in flight level can avoid a substantial fraction of contrails due to the shallowness of the ice-supersaturated layers (Figure 19). However, these results may exhibit a significant geographical variability depending on the prevalent synoptic situation and thus warrant further studies.

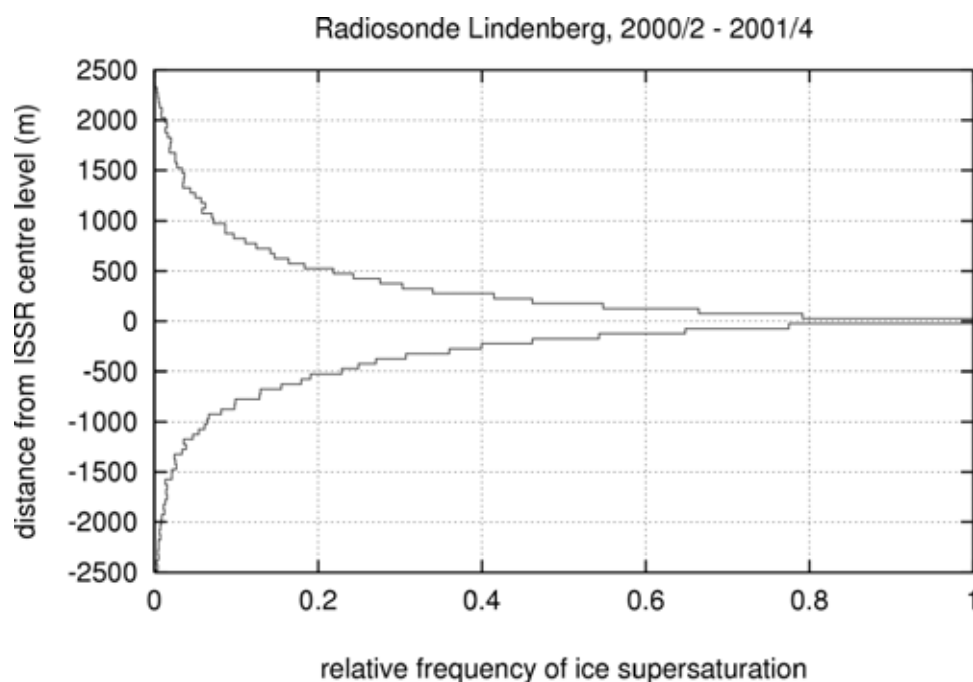


**Figure 19** Probability distribution of the vertical extent of layers of ice supersaturated air detected over Lindenberg. Thickness at FWHM of these layers is ~400 m.

A prerequisite for a strategy to avoid ice supersaturated regions is the ability of aviation weather forecasts to predict the location of such regions, an emerging field for which IPA paved the way with the updated ECMWF forecast system. Equipping commercial aircraft with humidity probes that are designed especially for use in the upper troposphere (including aircraft meteorological data reporting to weather centres) would allow more accurate predictions of ice-supersaturated regions. As air traffic density is lower during the night, when contrails have a large individual radiative forcing, there is a greater opportunity for redirecting flights out of ice supersaturated regions without dramatically enhancing the work load of air traffic controllers. The adoption of such routing only for aircraft producing the "worst" contrails would help make such a strategy affordable and keep fuel consumption penalties to a minimum. Whether such ideas can be implemented in operational flight routing without compromising safety is currently studied by IPA, Lufthansa and DWD in a joint BMBF project within the German Climate Protection Programme "klimazwei".

The impact of changing cruise altitudes on contrail coverage and corresponding radiative forcing was estimated in an ECHAM climate model study by means of global aircraft emission scenarios (developed within the EU project TRADEOFF), where cruise altitudes were displaced upward or downward globally by 2000 ft (~610 m) or multiples thereof.

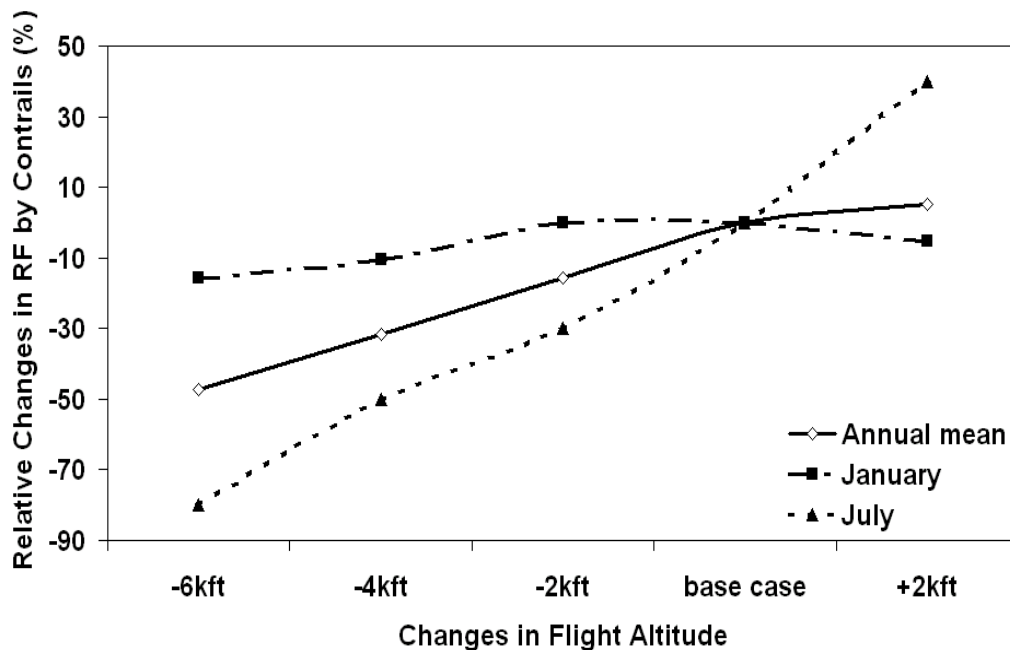


**Figure 20** Relative changes in global mean radiative forcing by line shaped contrails caused by changes in the mean flight altitude.

Based on the parameterization for line shaped contrails developed at IPA, changes in global mean radiative forcing of these contrails based on the discrete vertical displacements of air traffic are shown in Figure 20. Besides seasonal variations (compare January and July cases), considerable regional differences have been found; both are also noticeable in linear contrail coverage. These results are still uncertain and may underestimate the reduction of RF by flying higher because of a too moist lowermost model stratosphere. Regardless, they underscore the potential for reducing contrail effects by changes in cruise altitude.

### *Remote sensing reveals regional aviation impact on cirrus cloudiness*

Aircraft emissions of water vapor and particles trigger line-shaped contrails. In ice-supersaturated regions, contrails develop into long-lived contrail cirrus and lose their line shape, particularly in regions with large wind shear. The prevalence of high supersaturations with respect to ice in the upper troposphere heightens the importance of contrails in altering radiative forcing.

Satellite-based studies on the correlation between cirrus cloud cover and regional air traffic occurring at the same time have been carried out in PAZI-2. An increase of cirrus cover with air traffic density over Europe was found, see Figure 21. The increase in cirrus cover with traffic density was suggestive to be caused by contrail formation and spreading into contrail cirrus. However, the correlation can also be explained by the regional distribution of the natural cirrus coverage over Europe: Aircraft over Europe not only produce contrail cirrus; they also fly more often in areas with enhanced cirrus coverage. Hence, the result was not conclusive. Further work is ongoing to discriminate between contrail cirrus and natural cirrus.

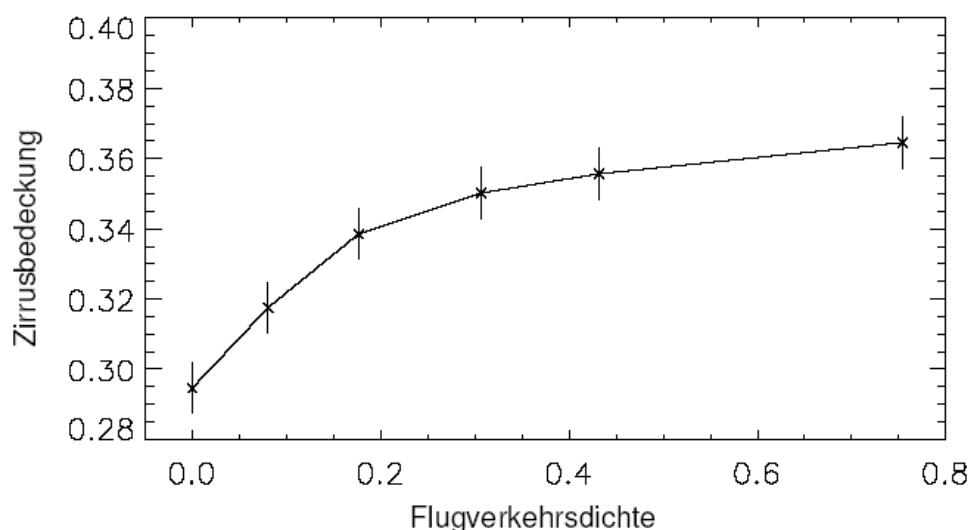


**Figure 21** Cirrus coverage derived from MSG as a function of air traffic density. Vertical bars depict the 95% statistical confidence level derived for individual air traffic density classes

### *New remote sensing data on coverage by linear contrails*

Within the ESA-DUE project "Contrails" the DLR contrail detection algorithm (CDA) was applied to satellite data of the years 1985, 1990, 1995, 2000 and 2004. For Europe and the North Atlantic (80° W – 50° E, 20° N – 75° N) the coverage by line shaped contrails is estimated from the AVHRR on NOAA-09, -11, -12, -14, -15, -16, and -17 and the ATSR2 and AATSR on ERS-2 and ENVISAT).

A rigorous validation against human interpretation of the satellite images made it possible to correct the data against the false alarm rate and the detection efficiency. Nevertheless, in areas with high air traffic density (Central Europe and US East coast) the coverage by linear contrails is underestimated, because many overlapping contrails are not detected by the algorithm.

*Climate model realizes contrail cirrus as an independent cloud type*

Until now contrail coverage was simply diagnosed from the atmospheric fields and from air traffic. Contrail coverage was then scaled to agree with observational data for line shaped contrails (those directly observable by satellites) over a specified area assuming the scaling constant to hold also in other areas. Contrails did not interact with the surrounding atmosphere. Figure 22 (top) shows the global annual mean contrail coverage that resulted from simulations with ECHAM using this parameterization.

Within PAZI-2, a process-based parameterization of contrails has been introduced that allows contrails to persist in the atmosphere and develop into contrail cirrus. The parameterization takes into account different processes that affect the contrail coverage and contrail ice water content. Contrails are advected away from the air traffic areas. Spreading due to vertical shear of the horizontal wind can considerably increase the spatial coverage. Contrails can accumulate ice mass due to deposition of water vapor competing with natural cirrus. They loose ice mass due to evaporation and precipitation.

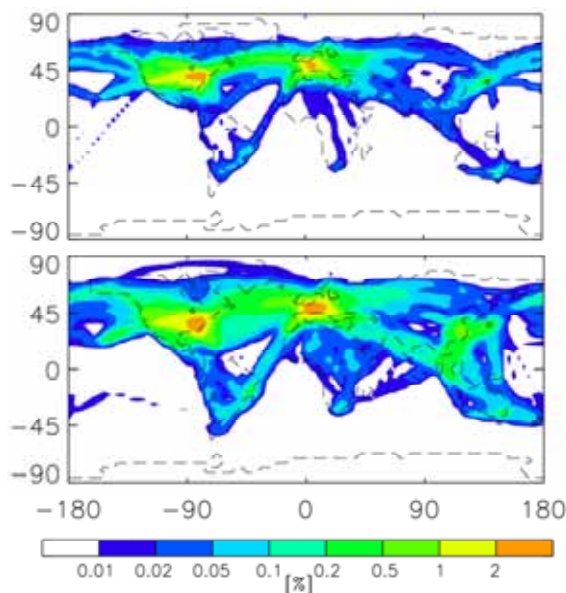


**Figure 22** Annual mean global contrail coverage from diagnosed line shaped contrails (top) and from contrails younger than 3 h using a new model version that includes contrail cirrus as an independent cloud type (bottom).

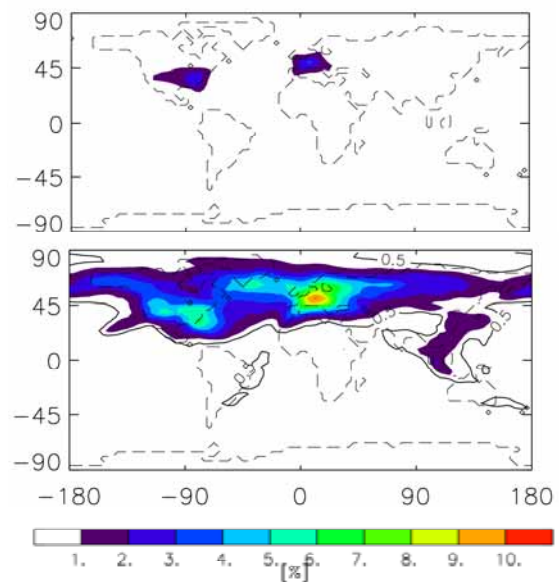


**Figure 23** Annual mean global coverage from contrails younger than ~3 h (top) and all contrails regardless of their age (bottom) obtained from the extended cloud scheme that explicitly simulates contrail cirrus life-cycles. Figures 22 (bottom) and 23 (top) are identical (note the change in color scale).

The temporal evolution of contrail coverage and contrail ice water content can now be simulated similar to the natural clouds and their ice water content. The new scheme allows for a separate evaluation of contrails of different ages. Comparing the contrails that are younger than ~3 hours (Figure 22 bottom) with the so-called line-shaped contrails of the old parameterization (top) it can be seen that the contrail coverage in the areas of maximum air traffic are similar and that due to advection contrail coverage simulated using the new parameterization can also be large away from the main air traffic routes. The main differences appear to be in the tropics where the new parameterization estimates higher contrail coverage than the old parameterization.

## Towards global estimates of contrail cirrus coverage

The spreading of contrails past the line shaped stage has not yet been studied in a global model. Therefore past estimates of aviation-induced cirrus had to rely on analysis of cirrus trends in regions with high air traffic density. Previous studies did not conclude on a best estimate of contrail cirrus coverage yet. With the extended ECHAM cloud scheme that includes contrail cirrus as a separate cloud type it is now possible to simulate aged contrails and their optical properties as well as young contrails.

First simulations suggest that contrail cirrus coverage can increase dramatically (Figure 23). Due to the interaction of contrails with the surrounding moisture field and due to the competition of contrails and natural cirrus for condensation, this increase in contrail cirrus is connected with a decrease in natural cirrus coverage. Nevertheless, contrail cirrus affect climate not only due to the additional cloud coverage but also due to the substitution of natural cirrus by contrail cirrus in case contrail cirrus are connected with slightly lower ice water contents and smaller effective radii. This again causes a different optical thickness of contrail cirrus compared to natural cirrus. These results are preliminary and require further validation. These topics will be studied in detail at IPA in the near future.

## Processes controlling cirrus clouds and the contrail-to-cirrus transition

A novel 2D/3D aerosol/cirrus microphysical code (LCM) has been set up that is based on the anelastic multiscale flow LES model EULAG. Using this innovative tool that includes Lagrangian ice particle tracking among other features, IPA participates in the most recent international GEWEX GCSS WG2 cirrus model intercomparison study. There, a suite of models are evaluated against a benchmark midlatitude cirrus case that is verified through a comprehensive set of in-situ and remote sensing measurements. The new model system EULAG-LCM will be used to elucidate critical hypotheses in cirrus cloud simulations and in support of field observations such as the planned HALO demonstration mission *ML-Cirrus* led by IPA.

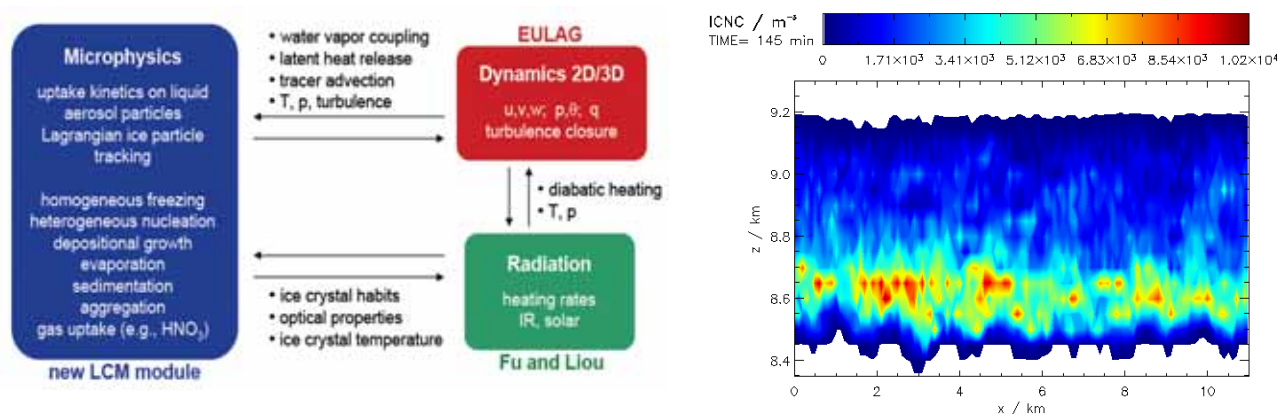


**Figure 24** Schematic illustration of the EULAG-LCM model system (left panel). Ice crystal number concentrations in a cirrus cloud initiated by gravity waves over a mountainous region from 2D LES simulations taken 145 min after the onset of heterogeneous ice nucleation (right panel). The spatial resolution is 50 m in the vertical and 100 m in the horizontal direction. Cloud evolution continues for several hours.

Figure 24 shows first EULAG-LCM ice crystal number concentrations (ICNC) for the 9 March 2000 benchmark case, an extended, long-lived cirrus forced by gravity waves over the Rocky Mountains. The highly resolved LES reveals the fine-scale structure of the in-cloud particle distribution developed at an early stage of cloud evolution. Resolved turbulent motions create regions of enhanced updrafts in the cloud, generating pockets of increased ice supersaturati-

ons. In these regions, the ICNC is larger than in surrounding areas. Making use of the LCM option to simulate different ice nucleation pathways, we were able to show, based on the measured ice water content of the cloud, that heterogeneous nucleation on a limited number of efficient IN is needed to explain the resulting cirrus cloud.

An efficient fluid dynamical model to study the evolution of contrails during the vortex phase has been developed using the LES-code EULAG along with a bulk microphysical scheme designed at IPA. This tool enables the quantification of a wide range of atmospheric and aircraft parameters describing the effects of vortex decay on contrail properties.

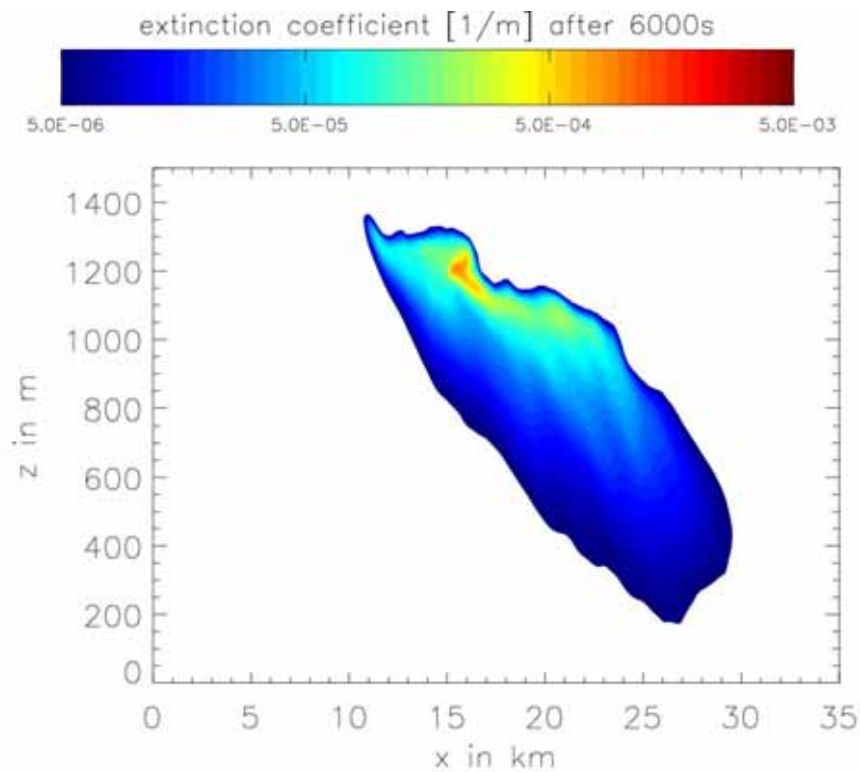


**Figure 25** Extinction coefficient of a 100 min old contrail in a stable atmosphere (217 K), at a relative humidity over ice of 120% and a vertical wind shear of 6 (m/s)/km.

Due to adiabatic heating in the sinking vortices, a considerable fraction of ice crystals is lost during the first few minutes of contrail development. Depending on relative humidity over ice (100-120%), only 0.3-30% of the initial number of crystals survive at 222 K at typical cruise altitudes. This may impact the subsequent contrail-to-cirrus transition, as the ice crystal concentration determines the depositional growth rate and consequently controls sedimentation. Currently, simulations of the contrail-to-cirrus transition are carried out (Figure 25). The relevance of parameters such as relative humidity, temperature and wind shear on optical, microphysical and geometric properties of contrail cirrus are investigated.

#### *Reduction of Cryoplane climate impact quantified*

Alternative fuels, if produced with low CO<sub>2</sub> emissions and low further environmental impact, may offer another possibility to reduce the aircraft climate impact significantly. One example is the use of liquid hydrogen as a fuel (cryoplane technology), which would reduce aircraft CO<sub>2</sub> emissions to zero. An assessment based on technology transition scenarios developed within the EU-project CRYOPLANE has been made. It includes the effects of all aircraft emission components, for which best estimates of their individual radiative forcing for present-day

conditions exist ( $\text{CO}_2$ , contrails,  $\text{NO}_x$ , and water vapor, but no contrail cirrus or soot-induced cirrus).

In case of a technology switch completed before 2065, and assuming that the required liquid hydrogen can be produced without additional fossil fuel burning, the potential of climate impact reduction is estimated by  $\sim 60\%$  in terms of radiative forcing in 2100. Due to the inertia of the climate system, the reduction potential is smaller, about 45%, in terms of surface temperature change in 2100.

### *Enhancing aviation-induced cloud cover: Aerodynamic contrails*

Figure 26 (top) shows a photo of a contrail-producing aircraft. However, the atmosphere was too warm for turbulent jet contrails to form (241 K at 300 hPa). In fact, a colorful, iridescent and laminar cloud sheet originates from the wing surfaces. After  $\sim 50$  m, this wing-induced aerodynamic contrail is captured by the expanding jet plumes, is mixed over the plume cross sections and begins to appear white.

Compressible fluid dynamics calculations carried out at IPA provided the flow field over the wings. This served as the basis to explain the appearance of aerodynamic contrails via dynamically induced aerosol particle freezing and ice condensation. The sequence of colors in the top figure suggests rapid growth of nearly mono-disperse ice particles in the visible size range, consistent with detailed microphysical-optical simulations shown in Figure 26 (bottom)

A simple time-scale analysis reveals that this new contrail type is favoured by high temperatures ( $> 230$  K) that are usually too warm for jet contrails to form. This implies an additional source of aircraft-induced ice particles in the upper troposphere, because contrail formation is now possible across a wider temperature range. Aerodynamic contrail properties and atmospheric relevance will be subject of future studies at IPA.

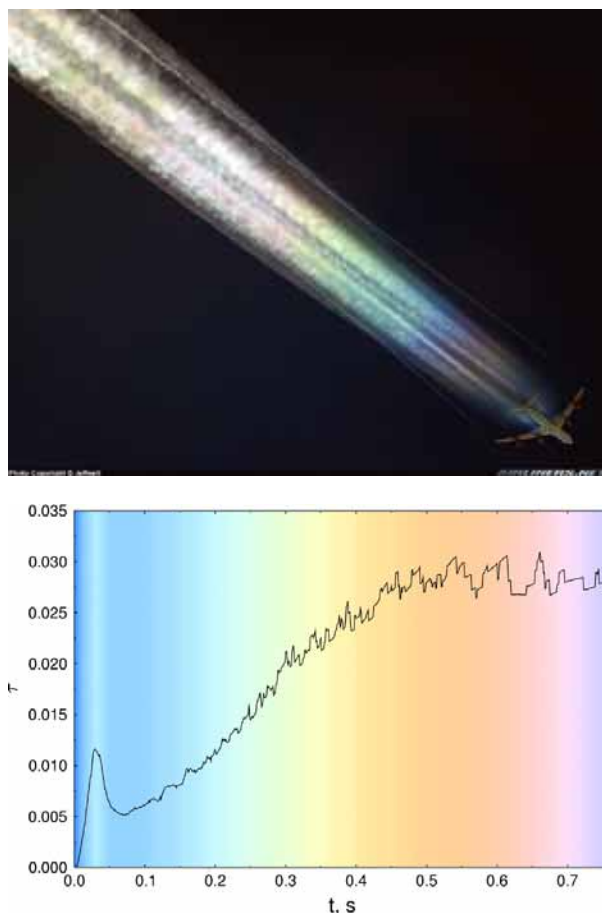


**Figure 26** Airbus A340 aircraft producing an aerodynamic contrail over eastern China (top photo courtesy of pilot and photographer Jeff Well). Bottom figure shows the calculated evolution of optical depth after the first ice crystals have formed. The underlying color sequence is consistent with the observation.

### *Heterogeneous chemistry in aircraft plumes—high sensitivity on local meteorology*

In collaboration with MPI Mainz and ETH Zurich in the framework of a doctoral thesis, an aircraft plume chemistry model has been developed on the basis of two coupled trajectory box models. Boxes describing plume and background processes are coupled by means of a mixing parameterization. Comprehensive gas phase chemistry for the tropopause region including acetone, ethane and their oxidation products is simulated. Heterogeneous halogen,  $N_2O_5$  and  $HO_x$  chemistry on various types of ambient and aircraft-induced particles is considered, using state-of-the-art solubility-dependent uptake coefficients for liquid-phase reactions. The microphysical scheme allows for coagulation, gas-diffusive particle growth and evaporation.

The chemical evolution from 1 s to 2 d after emission for contrail and non-contrail conditions has been studied in upper tropospheric and lowermost stratospheric conditions. Background conditions, such as relative humidity, local time of emission, and trace gas seasonal abundances have been varied. The results have been expressed in terms of effective emission (EEl) and perturbation (EPI) indices for the North Atlantic Flight Corridor. The results, especially for  $NO_y$  and  $O_3$ , are highly sensitive to the background conditions under which the emissions take place. The difference in EEl with and without considering plume processes indicates that these processes should not be neglected in parameterizations of plume chemistry in global models.

### *2.3 Overall summary*

#### *Soot effects and ice microphysics*

- Improved understanding of soot formation obtained from experimental studies using laboratory-scale flames (process studies) and using the HBK-S under more realistic thermodynamic conditions.
- Development of more reliable simulation techniques for combustion chambers enabling the prognostic treatment of physical properties of jet engine soot particles (THETA-Code).
- Refinement of methods employed to correlate physical properties of soot emissions from jet engines with different operating conditions for representative engines types.
- Substantial progress in parameterizing the aerosol-ice interaction in the climate model ECHAM4 through implementation of a scheme treating both homogeneous and heterogeneous ice nucleation consistently.
- Analysis and synthesis of ice nucleation behavior of soot particles from different sources including aircraft engines highlighted the difficulty to reconcile available laboratory data; it is unclear what makes soot particles efficient ice nucleating agents and whether aviation soot belongs to that category.
- First estimates of potential aircraft soot effects on cirrus with ECHAM4: depending on how background cirrus form, soot may lead to increases or decreases in ice crystal number density provided aircraft soot particles are good ice nuclei.

#### *Trace gas measurements and instrument development*

- Newly developed airborne measurement system based on chemical ionization mass spectrometry (ITCIMS) has been employed on the FALCON to derive vertical profiles of  $SO_2$  in various locations in support of model validation exercises.
- In-situ measurements of  $NO_y$  in cirrus clouds have been used to quantify the partitioning of reactive nitrogen: up to 30%  $HNO_3$  resides in cirrus ice particles at low temperatures.

### *Ice supersaturation and modeling of cirrus clouds*

- Ability to predict midlatitude cirrus properties from homogeneous ice nucleation has matured based on follow-on studies of this process in the aerosol/cloud chamber AIDA using an expanded set of liquid-containing particle precursors.
- Development and validation of a 2D/3D model system for the small-to-mesoscale Large-Eddy simulation of cirrus clouds using Lagrangian ice particle tracking and interactive aerosol microphysics.
- Analysis of humidity-corrected radiosondes in collaboration with the German Weather Service (DWD) yields insights into the vertical structure of ice supersaturated regions in the upper troposphere at midlatitudes.
- First quantification of moisture and temperature fluctuations along aircraft routes based on nine years of MOZAIC data.
- Implementation of ice supersaturation consistent with a prognostic cloud scheme in the European Centre for Medium Range Weather Forecasts (ECMWF) integrated forecast system led to improved relative humidity fields available in operational analyses.
- First near hemispheric, process-oriented simulations of aerosol effects on cirrus clouds quantify possible changes of cirrus properties and cirrus coverage due to heterogeneous ice nuclei.
- First thoughts on a statistical cirrus cloud scheme for the ECHAM5 general circulation model aiming at removing the basic inconsistency between resolved ice supersaturation, fractional coverage and ice microphysics.

### *Contrail cirrus, remote sensing and radiative transfer*

- Refinement of the radiative transfer code libRadtran with regard to the calculation of cirrus cloud radiative properties within the entire spectral region covered by MSG.
- New retrieval algorithm for cirrus clouds using MSG and comparison of the ECHAM4 radiation scheme with libRadtran.
- Remote sensing suggests possible correlation between regional air traffic over Europe and cirrus cloudiness, however, methods need to be refined.
- Measurement campaign PAZI-2/LAUNCH informed about properties of young contrails and their predictability with mesoscale and weather forecast models and yielded first perspectives on contrail mitigation.
- Development and validation of a 2D/3D Large-Eddy model system to simulate contrails and their transition into cirrus clouds.
- Introduction of contrail cirrus as a separate cloud type into the cloud scheme of the climate model ECHAM4, enabling for the first time the simulation of the life cycle of persistent contrails.
- First characterization of aerodynamically-induced contrails using a combination of fluid dynamical, microphysical and optical simulation tools.

## *2.4 New developments initiated by PAZI-2*

### *New condensed soot production mechanism and nano-soot generator available*

Because no reduced reaction mechanism for kerosene was obtained from the EU project SiA as originally planned, such a mechanism had to be developed at VT for the 3D combustor simulations. Due to the high computational demands, detailed mechanisms may not be used for complex 3D simulations. The base mechanism for a fuel consisting of 60% n-decane, 28% iso-octane, and 12% toluol comprises 151 species and 820 reactions. For a design pres-

sure of 10 bar, this mechanism was reduced to 72 species and 150 reactions. This still is a large mechanism but it enabled the simulation of the PAZI-2 combustor.

For the soot oxidation experiment a soot generator was needed. Based on the DLR-SOOT Generator (Patent DE 102 43 307 B4) a new generator with higher soot mass output for the controlled production of "nano soot particles" was developed, resulting in a German Patent Application DE 10 2005 010 766 A1. The soot generator can be used as a stable soot source for experiments where higher soot masses are needed.

#### *New HGF Junior Research Group AEROTROP focussing on aircraft-induced O<sub>3</sub>-changes*

The radiative forcing from aviation caused by CO<sub>2</sub> and NO<sub>x</sub>-induced ozone changes are, based on model results, of similar magnitude. Still experimental validation of the aircraft NO<sub>x</sub>-induced ozone changes are missing. There is little understanding of the interactions between gaseous aircraft NO<sub>x</sub> emissions and atmospheric particles, although cirrus abundance maximizes at aircraft cruise altitudes near the extratropical tropopause. Heterogeneous chemical processes are hardly considered in present estimates of aviation-induced climate change.

It is the aim of AEROTROP to investigate the impact of aircraft NO<sub>x</sub> emissions on the ozone chemistry of the tropopause region including particle processes in a holistic approach using aircraft measurements, satellite data and global modelling. The partitioning of reactive nitrogen species will be measured directly from aircraft in clear sky and cloudy conditions, and by chasing other aircraft. The data will serve as input for process studies to judge the relative importance of individual processes. Global model studies with ECHAM5 using coupled chemistry and aerosol-cirrus modules will help constrain or reduce uncertainties in aircraft NO<sub>x</sub>-induced ozone changes in climate projections.

#### *New statistical cloud scheme for ECHAM5*

New ECHAM4 model developments (to be transferred to ECHAM5 in the near future) included parameterizations for homogeneous freezing and heterogeneous ice nucleation in cirrus clouds allowing for explicit (grid-scale) ice supersaturation, and contrail cirrus. The climate effect of the former cannot be conclusively determined since the cirrus coverage is not consistent with the supersaturation. The latter could not yet be based on the new microphysical parameterizations because of this inconsistency between supersaturation and cloud coverage.

To make progress and eventually obtain a unified global model system as far as cloud and radiation modules are concerned, enabling a physically-based simultaneous treatment of contrail and soot effects, we have begun to build up scientific expertise in the area of statistical cloud modeling. It is planned to formulate and introduce a novel cloud coverage formulation in ECHAM5 that will be consistent with explicit supersaturation and would therefore allow for the estimation of the climate impact of the indirect aerosol effect on cirrus. To simulate non-equilibrium conditions this cloud coverage needs to be prognostic. It is further planned to use the cloud scheme as implemented in the ECMWF integrated forecast system and to modify this prognostic scheme for cirrus. Only in such a model environment can cirrus and contrail cirrus be treated consistently.

*New fast assessment tool to evaluate aviation climate impact*

Aviation-induced climate change is a challenge to society. To cope with this challenge, assessment tools are needed that are suitable to evaluate new technology options with respect to their potential climate impact. Such a tool (AirClim) has been developed at IPA within the EU-Integrated Project HISAC focusing on supersonic transport.

AirClim estimates the temporal development of the climate impact caused by aircraft emissions by means of linearization of processes (transport, chemistry, radiation) occurring from the emission to changes in the globally mean near surface temperature. AirClim was designed for aircraft technology applications and takes into account changes in CO<sub>2</sub>, H<sub>2</sub>O, CH<sub>4</sub> and O<sub>3</sub> (the latter two resulting from NO<sub>x</sub> emissions) as well as line-shaped contrails. Basic inputs are pre-calculated atmospheric data using a detailed state-of-the-art climate-chemistry-model and aircraft-emission data sets. AirClim will be modified to deal with subsonic fleets.



## Appendix: List of research publications (as of December 2007)

### Atmospheric research

- Abbatt, J.P.D., S. Benz, D.J. Cziczo, Z. Kanji, U. Lohmann, and O. Möhler  
Solid ammonium sulfate aerosols as ice nuclei: A pathway for cirrus cloud formation.  
*Science* 313 (5794), 1770-1773, 2006.
- Cotton, R.J., S. Benz, P.R. Field, O. Möhler, and M. Schnaiter  
Technical note: A numerical test-bed for detailed ice nucleation studies in the AIDA cloud simulation chamber.  
*Atmos. Chem. Phys.* 7, 243-256, 2007.
- Dietmüller, S., M. Ponater, R. Sausen, K.-P. Hoinka, and S. Pechtl  
Contrails, natural clouds, and diurnal temperature range.  
*J. Clim.*, submitted, 2007.
- Dotzek, N. and K. Gierens  
Instantaneous fluctuations of temperature and moisture in the upper troposphere and tropopause region. Part 2: Structure functions and intermittency.  
*Meteorol. Z.*, submitted, 2007.
- Emde, C. and B. Mayer  
Simulation of solar radiation during a total eclipse: a challenge for radiative transfer.  
*Atmos. Chem. Phys.* 7, 2259-2270, 2007.
- Feldpausch, Ph., M. Fiebig, L. Fritzsche, and A. Petzold  
Measurement of ultrafine aerosol size distributions by a diffusion separator-CPC combination.  
*J. Aerosol Sci.* 36, 2005.
- Fichter, C., S. Marquart, R. Sausen, and D.S. Lee  
The impact of cruise altitude on contrails and related radiative forcing.  
*Meteorol. Z.* 14, 563-572, 2005.
- Fiebig, M., C. Stein, F. Schröder, P. Feldpausch, and A. Petzold  
Inversion of data containing information on the aerosol particle size distribution using multiple instruments.  
*J. Aerosol Sci.* 36, 1353-1372, 2005.
- Field, P., O. Möhler, P. Connolly, M. Krämer, R. Cotton, A. Heymsfield, H. Saathoff, and M. Schnaiter  
Some ice nucleation characteristics of Asian and Saharan desert dust.  
*Atmos. Chem. Phys.* 6, 2991-3006, 2006.
- Gayet, J.-F., J. Ovarlez, V. Shcherbakov, J. Ström, U. Schumann, A. Minikin, F. Auriol, A. Petzold and M. Monier  
Cirrus cloud microphysical and optical properties at southern and northern midlatitudes during the INCA experiment.  
*J. Geophys. Res.* 109, D20206, doi:10.1029/2004JD004803, 2004.
- Gayet, J.-F., V. Shcherbakov, H. Mannstein, A. Minikin, U. Schumann, J. Ström, A. Petzold, J. Ovarlez, and F. Immler  
Microphysical and optical properties of midlatitudes cirrus clouds observed in the southern hemisphere during INCA.  
*Q. J. R. Meteorol. Soc.* 132, 1-30, 2006.
- Gierens, K., and U. Schumann  
Ice-supersaturation in the upper troposphere.  
*GEWEX News* 14, 6-7, 2004.
- Gierens, K., R. Kohlhepp, N. Dotzek, and H.G.J. Smit  
Instantaneous fluctuations of temperature and moisture in the upper troposphere and tropopause region. Part 1: Probability densities and their variability.  
*Meteorol. Z.* 16, 221-231, 2007.
- Haag, W. and B. Kärcher  
The impact of aerosols and gravity waves on cirrus clouds at midlatitudes.  
*J. Geophys. Res.* 109, D12202, doi:10.1029/2004JD004579, 2004.

- Hendricks, J., B. Kärcher, A. Döpelheuer, J. Feichter, U. Lohmann, and D. Baumgardner  
Simulating the global atmospheric black carbon cycle: A revisit to the contribution of aircraft emissions.  
*Atmos. Chem. Phys.* 4, 2521-2541, 2004.
- Hendricks, J., B. Kärcher, M. Ponater, and U. Lohmann  
Do aircraft black carbon emissions affect cirrus clouds on a global scale?  
*Geophys. Res. Lett.* 32, L12814, doi:10.1029/2005GL022740, 2005.
- Huntrieser, H., U. Schumann, H. Schlager, H. Höller, A. Giez, H. D. Betz, D. Brunner, C. Forster, O. Pinto Jr., and R. Calheiros  
Lightning activity in Brazilian thunderstorms during TROCCINOX: Implications for NO<sub>x</sub> production  
*Atmos. Chem. Phys. Disc.* 7, 14813-14894, 2007.
- Joos, H., P. Spichtinger, U. Lohmann, J.-F. Gayet, and A. Minikin  
Orographic cirrus in the global climate model ECHAM5.  
*J. Geophys. Res.*, submitted, 2007.
- Kärcher, B.  
Supersaturation, dehydration, and denitrification in Arctic cirrus.  
*Atmos. Chem. Phys.* 5, 1757-1772, 2005.
- Kärcher, B. and M.M. Basko  
Trapping of trace gases in growing ice crystals.  
*J. Geophys. Res.*, 109, D22204, doi:10.1029/2004JD005254, 2004.
- Kärcher, B. and T. Koop  
The role of organic aerosols in homogeneous ice formation.  
*Atmos. Chem. Phys.* 5, 703-714, 2005.
- Kärcher, B. and C. Voigt  
Formation of nitric acid/water ice particles in cirrus clouds.  
*Geophys. Res. Lett.* 33, L08806, doi:10.1029/2006GL025927, 2006.
- Kärcher, B., J. Hendricks, and U. Lohmann  
Physically-based parameterization of cirrus cloud formation for use in global atmospheric models.  
*J. Geophys. Res.* 111, D01205, doi:10.1029/2005JD006219, 2006.
- Kärcher, B., O. Möhler, P.J. DeMott, S. Pechtl, and F. Yu  
Insights into the role of soot aerosols in cirrus cloud formation.  
*Atmos. Chem. Phys.* 7, 4203-4227, 2007.
- Kärcher, B. and U. Burkhardt  
Prediction of cirrus clouds in general circulation models.  
*Q. J. R. Meteorol. Soc.*, submitted, 2007.
- Kinne, S., M. Schulz, C. Textor, S. Guibert, Y. Balkanski, S. E. Bauer, T. Berntsen, T. F. Berglen, O. Boucher, M. Chin, W. Collins, F. Dentener, T. Diehl, R. Easter, J. Feichter, D. Fillmore, S. Ghan, P. Ginoux, S. Gong, A. Grini, J. Hendricks, M. Herzog, L. Horowitz, I. Isaksen, T. Iversen, A. Kirkevåg, S. Kloster, D. Koch, J. E. Kristjansson, M. Krol, A. Lauer, J. F. Lamarque, G. Lesins, X. Liu, U. Lohmann, V. Montanaro, G. Myhre, J. Penner, G. Pitari, S. Reddy, O. Seland, P. Stier, T. Takemura, and X. Tie  
An AeroCom initial assessment – optical properties in aerosol component modules of global models.  
*Atmos. Chem. Phys.* 6, 1815-1834, 2006.
- Krüger, V., C. Wahl, R. Hadeff, K.P. Geigle, W. Stricker, and M. Aigner  
Comparison of laser-induced incandescence method with scanning mobility particle sizer technique: the influence of probe sampling and laser heating to soot particle size distribution.  
*Measurement Sci. Technol.* 16, 1477-1486, 2005.
- Law, K., L. Pan, H. Wernli, H. Fischer, P. Haynes, R. Salawitch, B. Kärcher, M. Prather, S. Doherty, and A.R. Ravishankara  
Processes governing the chemical composition of the extra-tropical UTLS.  
*IGAC Newsletter No.* 32, 2-22, 2005.

- Lauer, A., J. Hendricks, J. Feichter, I. Ackermann, B. Schell, H. Hass, and S. Metzger  
Simulating aerosol microphysics with the ECHAM/MADE GCM - Part I: Model description and comparison with observations.  
*Atmos. Chem. Phys.* 5, 3251-3276, 2005.
- Lauer, A., and J. Hendricks  
Simulating aerosol microphysics with the ECHAM4/MADE GCM – Part II: Results from a first multiannual simulation of the submicrometer aerosol.  
*Atmos. Chem. Phys.* 6, 5495-5513, 2006.
- Lohmann, U., B. Kärcher, and J. Hendricks  
Sensitivity studies of cirrus clouds formed by heterogeneous freezing in the ECHAM GCM.  
*J. Geophys. Res.* 109, D16204, doi:10.1029/2003JD004443, 2004.
- Mangold, A., R. Wagner, H. Saathoff, U. Schurath, C. Giesemann, V. Ebert, M. Krämer, O. Möhler  
Experimental investigation of ice nucleation by different types of aerosols in the aerosol chamber AIDA: implications to microphysics of cirrus clouds.  
*Meteorol. Z.* 14, 485-497, 2005.
- Mannstein, H. and U. Schumann  
Aircraft induced contrail cirrus over Europe.  
*Meteorol. Z.* 14, 549-554, 2005. (Corrigendum: *Meteorol. Z.* 16, 131-132, 2007).
- Mayer, B. and A. Kylling  
Technical note: The libRadtran software package for radiative transfer calculations - description and examples of use.  
*Atmos. Chem. Phys.* 5, 1855-1877, 2005.
- Meilinger, S.K., B. Kärcher, and Th. Peter  
Microphysics and heterogeneous chemistry in aircraft plumes - High sensitivity on local meteorology and atmospheric composition.  
*Atmos. Chem. Phys.* 5, 533-545, 2005.
- Minnis, P., R. Palikonda, B.J. Walther, J.K. Ayers, and H. Mannstein  
Contrail properties over the Eastern North Pacific from AVHRR data.  
*Meteorol. Z.* 14, 515-523, 2005.
- Möhler, O., C. Linke, H. Saathoff, M. Schnaiter, R. Wagner, A. Mangold, M. Krämer, and U. Schurath  
Ice nucleation on flame soot aerosol of different organic carbon content.  
*Meteorol. Z.* 14, 477-484, 2005.
- Möhler, O., S. Büttner, C. Linke, M. Schnaiter, H. Saathoff, O. Stetzer, R. Wagner, M. Krämer, A. Mangold, V. Ebert, and U. Schurath  
Effect of sulphuric acid coating on heterogeneous ice nucleation by soot aerosol particles.  
*J. Geophys. Res.* 110, D11210, doi:10.1029/2004JD005169, 2005.
- Möhler, O., P.R. Field, P. Connolly, S. Benz, H. Saathoff, M. Schnaiter, R. Wagner, R. Cotton, M. Krämer, A. Mangold, and A.J. Heymsfield  
Efficiency of the deposition mode ice nucleation on mineral dust particles.  
*Atmos. Chem. Phys.* 6, 3007-3021, 2006.
- Palikonda, R., P. Minnis, D.P. Duda, and H. Mannstein  
Contrail coverage derived from 2001 AVHRR data over the continental United States of America and surrounding areas.  
*Meteorol. Z.* 14, 525-536, 2005.
- Petzold, A., M. Fiebig, L. Fritzsche, C. Stein, U. Schumann, C. W. Wilson, C. D. Hurley, F. Arnold, E. Katragkou, U. Baltensperger, M. Gysel, S. Nyeki, R. Hitzenberger, H. Giebl, K. J. Hughes, R. Kurtenbach, P. Wiesen, P. Madden, H. Puxbaum, S. Vrchoticky, and C. Wahl  
Particle emissions from aircraft engines – a survey of the European project PartEmis.  
*Meteorol. Z.* 14, 465-476, 2005.
- Ponater M., S. Marquart, R. Sausen, and U. Schumann  
On contrail climate sensitivity.  
*Geophys. Res. Lett.* 32, L10706, doi:10.1029/2005GL022580, 2005.

- Ponater, M. S. Pechtl, R. Sausen, U. Schumann, and G. Hüttig  
Potential of the cryoplane technology to reduce aircraft climate impact: A state-of-the-art assessment.  
*Atmos. Environ.* 40, 6928–6944, 2006.
- Popp, P.J., T.P. Marcy, E.J. Jensen, B. Kärcher, D.W. Fahey, R.S. Gao, T.L. Thompson, K.H. Rosenlof, E.C. Richard, R.L. Herman, E.M. Weinstock, J.B. Smith, R.D. May, H. Vömel, J.C. Wilson, A.J. Heymsfield, M.J. Mahoney, and A.M. Thompson  
The observation of nitric acid-containing particles in the tropical lower stratosphere.  
*Atmos. Chem. Phys.* 6, 601–611, 2006.
- Popp, P.J., T.P. Marcy, L.A. Watts, R.S. Gao, D.W. Fahey, E.M. Weinstock, J.B. Smith, R.L. Herman, R.F. Troy, C.R. Webster, L.E. Christensen, D.G. Baumgardner, C. Voigt, B. Kärcher, J.C. Wilson, M.J. Mahoney, E.J. Jensen, and T.P. Bui  
Condensed-phase nitric acid in a tropical subvisible cirrus cloud.  
*Geophys. Res. Lett.*, 34, L24812, doi:10.1029/2007GL031832, 2007.
- Sausen, R., I. Isaksen, V. Grewe, D. Hauglustaine, D.S. Lee, G. Myhre, M.O. Köhler, G. Pitari, U. Schumann, F. Stordal, and C. Zerefos  
Aviation radiative forcing in 2000: An update on IPCC (1999).  
*Meteorol. Z.* 14, 555–561, 2005.
- Schneider, J., N. Hock, S. Hings, S. Weimer, S. Borrmann, M. Fiebig, A. Petzold, R. Busen, B. Kärcher  
Aircraft-based mass spectrometric aerosol measurements: Chemical composition of tropospheric background aerosol and aircraft exhaust particles.  
*J. Aerosol Sci.* 37, 839–857, 2006.
- Schumann, U.  
Formation, properties and climatic effects of contrails.  
*C. R. Physique* 6, 549–565, 2005.
- Schumann, U., and H. Huntrieser  
The global lightning-induced nitrogen oxides source.  
*Atmos. Chem. Phys.* 7, 3823–3907, 2007.
- Schwarz, J.P., R.S. Gao, D.W. Fahey, D.S. Thomson, L.A. Watts, J.C. Wilson, J.M. Reeves, M. Darbeheshti, D.G. Baumgardner, G.L. Kok, S.H. Chung, M. Schulz, J. Hendricks, A. Lauer, B. Kärcher, J.G. Slowik, K.H. Rosenlof, T.L. Thompson, A.O. Langford, M. Loewenstein, K.C. Aikin  
Single particle measurements of mid latitude black carbon and light-scattering aerosols from the boundary layer to the lower stratosphere.  
*J. Geophys. Res.* 111, D16207, doi:10.1029/2006JD007076, 2006.
- Seifert, M., J. Ström, R. Krejci, A. Minikin, A. Petzold, J.-F. Gayet, H. Schlager, H. Ziereis, U. Schumann and J. Ovarlez  
Thermal stability analysis of particles incorporated in cirrus crystals and of non activated particles in between the cirrus crystals: Comparing clean and polluted air masses.  
*Atmos. Chem. Phys.* 4, 1343–1353, 2004.
- Shcherbakov, V., J.-F. Gayet, O. Jourdan, J. Ström, and A. Minikin  
Light scattering by single ice crystals of cirrus clouds.  
*Geophys. Res. Lett.*, 33, L15809, doi:10.1029/2006GL026055, 2006.
- Speidel, M., R. Nau, F. Arnold, H. Schlager, and A. Stohl  
Sulfur dioxide measurements in the lower, middle, and upper troposphere: Deployment of an aircraft-based chemical ionization mass spectrometer with permanent in-flight calibration.  
*Atmos. Environ.* 41, 2427–2437, 2007.
- Somnitz, H., G.G. Gleitsmann, and R. Zellner  
Novel rates of OH induced sulfur oxidation. Implications to the plume chemistry of jet aircraft.  
*Meteorol. Z.* 14, 459–464, 2005.
- Sorokin, A., E. Katragkou, F. Arnold, R. Busen, and U. Schumann  
Gaseous SO<sub>3</sub> and H<sub>2</sub>SO<sub>4</sub> in the exhaust of an aircraft gas turbine engine: measurements by CIMS and implications for fuel sulfur conversion to sulfur (VI) and conversion of SO<sub>3</sub> to H<sub>2</sub>SO<sub>4</sub>.  
*Atmos. Environ.* 38 449–456, 2004.

- Starik, A.M., A.M. Savel'ev, N.S. Titiva, E.E. Loukhovitskaya, and U. Schumann  
Effect of aerosol precursors from gas turbine engines on the volatile sulfate aerosols and ion clusters formation in aircraft plumes.  
*Phys. Chem. Chem. Phys.* 6, 3426-3436, 2004.
- Stubenrauch C.J., and U. Schumann  
Impact of air traffic on cirrus coverage.  
*Geophys. Res. Lett.* 32, L14813, doi:10.1029/2005GL022707, 2005.
- Textor, C., M. Schulz, S. Guibert, S. Kinne, Y. Balkanski, S. Bauer, T. Berntsen, T. Berglen, O. Boucher, M. Chin, F. Dentener, T. Diehl, R. Easter, H. Feichter, D. Fillmore, S. Ghan, P. Ginoux, S. Gong, A. Grini, J. Hendricks, L. Horowitz, P. Huang, I. Isaksen, T. Iversen, S. Kloster, D. Koch, A. Kirkevåg, J.E. Kristjansson, M. Krol, A. Lauer, J.F. Lamarque, X. Liu, V. Montanaro, G. Myhre, J. Penner, G. Pitari, S. Reddy, Ø. Seland, P. Stier, T. Takemura, and X. Tie  
Analysis and quantification of the diversities of aerosol life cycles within AeroCom.  
*Atmos. Chem. Phys.* 6, 1777-1813, 2006.
- Textor, C., M. Schulz, S. Guibert, S. Kinne, Y. Balkanski, S. Bauer, T. Berntsen, T. Berglen, O. Boucher, M. Chin, F. Dentener, T. Diehl, J. Feichter, D. Fillmore, P. Ginoux, S. Gong, A. Grini, J. Hendricks, L. Horowitz, P. Huang, I. S. A. Isaksen, T. Iversen, S. Kloster, D. Koch, A. Kirkevåg, J. E. Kristjansson, M. Krol, A. Lauer, J. F. Lamarque, X. Liu, V. Montanaro, G. Myhre, J. E. Penner, G. Pitari, M. S. Reddy, Ø. Seland, P. Stier, T. Takemura, and X. Tie  
The effect of harmonized emissions on aerosol properties in global models – an AeroCom experiment.  
*Atmos. Chem. Phys.* 7, 4489-4501, 2007.
- Tompkins, A., K. Gierens, and G. Rädcl  
Ice supersaturation in the ECMWF Integrated Forecast System.  
*Q. J. R. Meteorol. Soc.* 133, 53-63, 2007.
- Unterstrasser, S., K. Gierens, and P. Spichtinger  
The evolution of contrail microphysics and structure in the vortex phase.  
*Meteorol. Z.*, accepted, 2007.
- Voigt, C., H. Schlager, H. Ziereis, B. Kärcher, B.P. Luo, C. Schiller, M. Krämer, H. Irie, Y. Kondo, and P. Popp  
Nitric acid uptake in cirrus clouds.  
*Geophys. Res. Lett.* 33, L05803, doi:10.1029/2005GL025159, 2006.
- Voigt, C., B. Kärcher, H. Schlager, C. Schiller, M. Krämer, M. de Reus, H. Vössing, S. Borrmann, and V. Mitev  
In-situ observations and modeling of small nitric acid-containing ice crystals.  
*Atmos. Chem. Phys.* 7, 3373-3383, 2007.
- Wagner, R., S. Benz, O. Möhler, H. Saathoff, M. Schnaiter, and T. Leisner  
Influence of particle aspect ratio on the midinfrared extinction spectra of wavelength-sized ice crystals.  
*J. Phys. Chem. A* 111, 13,003-13,022, 2007.
- Wilson, C.W., A. Petzold, S. Nyeki, U. Schumann, and R. Zellner  
Measurement and prediction of emissions of aerosols and gaseous precursors from gas turbine engines (PartEmis): An overview.  
*Aerosp. Sci. Technol.* 8, 131-143, 2004.
- Ziereis, H., A. Minikin, H. Schlager, J. F. Gayet, F. Auriol, P. Stock, J. Baehr, A. Petzold, U. Schumann, A. Weinheimer, B. Ridley, and J. Ström  
Uptake of reactive nitrogen on cirrus cloud particles during INCA.  
*Geophys. Res. Lett.* 31, L05115 10.1029/2003GL018794, 2004.

Soot research

- Di Domenico, M., P. Gerlinger, and M. Aigner  
Detailed Soot Formation Model in Flames.  
Proceedings of the European Combustion Meeting, 2005.
- Di Domenico, M., P. Gerlinger, and M. Aigner  
Modeling Soot Formation in Methane Diffusion Flames.  
AIAA paper 2006-1163, 2006.
- Di Domenico, M., P. Gerlinger, and M. Aigner  
Modeling Soot Formation in Laminar Ethylene-Air Diffusion Flames.  
42<sup>nd</sup> AIAA/ASME/SAE/ASEE Joint Propulsion Conference and Exhibit, 2006.
- Di Domenico, M., P. Gerlinger, and M. Aigner  
Numerical Investigation of Soot Formation in Partially- Premixed Diffusion Flames  
31<sup>st</sup> International Symposium on Combustion, 2006.
- Di Domenico, M., P. Gerlinger, and M. Aigner  
Chemistry and Turbulence Modeling Effects on the Numerical Simulation of Lifted H<sub>2</sub>/N<sub>2</sub>  
Flames in Vitiated Coflow  
37<sup>th</sup> AIAA Fluid Dynamics Conference and Exhibit, 2007.
- Di Domenico, M., P. Gerlinger, and M. Aigner  
Numerical Investigation of Soot Formation in Laminar Ethylene-Air Diffusion Flames.  
ASME paper GT2007-27118, 2007.
- Geigle, K.P., Y. Schneider-Kühnle, M. Tsurikov, R. Hedef, R. Lückcrath, V. Krüger, W. Stricker, and M. Aigner  
Investigation of laminar pressurized flames for soot model validation using SV-CARS and LII.  
Proceedings International Symposium on Combustion, Vol. 30, 1645-1653, 2005.
- Geigle, K.P., M.S. Tsurikov, W. Meier, V. Krüger, and R. Hedef  
Laser-induced incandescence and shifted vibrational CARS in laminar premixed flames at atmospheric and elevated pressures.  
Proceedings of the International Bunsen Discussion Meeting and Workshop on Laser-induced incandescence, 2005.
- Geigle, K.P., O. Lammel, A. Koch, R. Stirn, and W. Meier  
Soot volume fraction study by laser-induced incandescence in a technical scale aero-engine combustor up to 15 bar  
31<sup>st</sup> International Symposium on Combustion, 2006.
- Kanjarkar, S., C. Wahl, and M. Aigner  
Investigation of Nano-Soot Particle Oxidation in a Flow Reactor.  
9<sup>th</sup> International ETH-Conference on Combustion-Generated Particles, 2005.
- Kanjarkar, S., C. Wahl, M. Kapernaum, M., and M. Aigner  
Investigation of Nano-Soot Particle Oxidation in a Flow Reactor Experimental investigation of soot nanoparticle oxidation –Effect of oxygen partial pressure on reaction kinetics  
31<sup>st</sup> International Symposium on Combustion, 2006.
- Krüger, V., K.P. Geigle, Y. Schneider-Kühnle, R. Hedef, M. Tsurikov, and M. Aigner  
Mesure par LII de la concentration et de la taille de la suie dans une flamme prémélangée la minaire.  
12. Congres Français de Mécanique (CFM), 2005.
- Slavinskaya, N.A  
Skeletal Mechanism for Kerosene Combustion with PAH Production.  
AIAA paper 2000-0992, 2008.
- Slavinskaya, N.A, and C. Lenfers  
Skeletal Mechanism for n-Decane.  
2<sup>nd</sup> International Workshop on Model Reduction in Reacting Flow, Rome, Italy, 2007.
- Schneider-Kühnle, Y., K.P. Geigle, V. Krüger, R. Lückcrath, M. Tsurikov, W. Stricker, and M. Aigner  
Development of a Shifted-Vibrational N<sub>2</sub>-CARS System and Application to Pressurized Sooting Flames.  
ECONOS 2004, Erlangen, Germany, 2004.

- Tsurikov, M.V., K.P. Geigle, V. Krüger, Y. Schneider-Kühnle, W. Stricker, R. Lückerrath, R. Hadeff, and M. Aigner  
Laser-based Investigation of Soot Formation in Laminar Premixed Flames at Atmospheric and Elevated Pressures Investigation of Nano-Soot Particle Oxidation in a Flow Reactor.  
Combustion Sci. Technol. 177, 1635-1862, 2005.
- Wahl, C.  
Variabler Nanosoot-Generator als stabile und reproduzierbare Verbrennungsrußquelle z.B. zur Filterprüfung.  
Symposium der Palas GmbH, Daimler Chrysler Werk, Wörth, February 2004.
- Wahl, C., M. Kapernaum, Th. Rindlisbacher, and W. Bula  
Nanoparticle Emissions of a small Piston- Engine powered Aircraft.  
8<sup>th</sup> International ETH-Conference on Combustion Generated Particles, Zürich, Switzerland, 2004.
- Wahl, C., M. Kapernaum, H. Zaafar, M. Aigner, Th. Rindlisbacher, W. Bula, and L. Hjelmberg  
Nanoparticle Emissions of Flight Engines.  
ASME paper GT2005-68757, 2005.
- Wahl, C., Th. Rindlisbacher, and L. Hjelmberg  
Microphysical and chemical properties of nanoparticles emitted by flight engines.  
24<sup>th</sup> Annual AAAR Conference, 2005.
- Wahl, C., H. Jaafar jr., and M. Kapernaum  
Soot formation and identification of soot precursors in a fuel rich ethylene flame.  
9<sup>th</sup> International ETH-Conference on Combustion Generated Particles, 2005.
- Wahl, C., M. Kapernaum, and Th. Rindlisbacher  
Separation of Aircraft and Diesel-Truck Particle-Emissions, a Contribution to Airport Air Quality Measurements.  
10<sup>th</sup> ETH-Conference on Combustion Generated Nanoparticles, 2006.
- Wahl, C., M. Kapernaum, and Th. Rindlisbacher  
Comparison of Nanoparticle Formation Caused by Leaded and Unleaded Aviation Gasoline Combustion.  
11<sup>th</sup> ETH-Conference on Combustion Generated Nanoparticles, 2007.

### Planned publications

- Arnold, F., T. Schuck, T. Pirjola, R. Nau, H. Schlager, V. Fiedler, A. Minikin, and A. Stohl  
Upper tropospheric SO<sub>2</sub> pollution over South America: Impact on aerosol and cloud condensation nuclei formation.  
Atmos. Chem. Phys., in preparation, 2007.
- Burkhardt, U., B. Kärcher, M. Ponater, and K. Gierens  
Contrail cirrus supporting areas.  
Geophys. Res. Lett., in preparation, 2007.
- Burkhardt, U., and B. Kärcher  
Parameterization of contrail cirrus in GCMs.  
J. Geophys. Res., in preparation, 2007.
- Febvre, G., J.-F. Gayet, B. Kärcher, A. Minikin, V. Shcherbakov, O. Jourdan, U. Schumann, H. Schlager, R. Busen, and M. Fiebig  
On optical and microphysical characteristics of contrails and cirrus.  
J. Geophys. Res., in preparation, 2007
- Fiedler, V., F. Arnold, H. Schlager, A. Minikin, and S. Ludmann  
Acidic trace gases in an aged tropical biomass burning plume: Aircraft based CIMS measurements and implication for soot activation.  
Atmos. Chem. Phys., in preparation, 2007.
- Gierens, K., B. Kärcher, H. Mannstein, and B. Mayer  
Aerodynamic contrails: Phenomenology and flow physics.  
J. Atmos. Sci., in preparation, 2007.

- Kärcher, B., B. Mayer, K. Gierens, U. Burkhardt, H. Mannstein, and R. Chatterjee  
Aerodynamic contrails: Microphysics and optical properties.  
J. Atmos. Sci., in preparation, 2007.
- Schuck, T., F. Arnold, R. Nau, V. Fiedler, M. Speidel, and H. Schlager  
First aircraft-based measurements of sulfur dioxide in the upper troposphere over South America.  
Atmos. Chem. Phys., in preparation, 2007.

### Theses

- Di Domenico, M.  
Numerical Simulation of Soot Formation in Turbulent Flows. Dissertation, Universität Stuttgart, 2007.
- Fiedler, V.  
Atmospheric SO<sub>2</sub>: Global measurements using aircraft-based CIMS. Dissertation, Universität Heidelberg, 2007.
- Haag, W.  
Zur Initiierung der Eisphase in Zirruswolken: Numerische Simulationen von Gefrierprozessen in einer Aerosolkammer und atmosphärische Implikationen. Dissertation, Universität München, DLR-FB 2004-04, 2004.
- Krebs, W.  
Analyse des Einflusses des Flugverkehrs auf die natürliche Zirrusbewölkung über Europa, Nordafrika und dem Nordatlantik. Dissertation, Universität München, DLR-FB 2006-10, 2006.
- Kurz, C.  
Entwicklung und Anwendung eines gekoppelten Klima-Chemie-Modellsystems. Dissertation, Universität München, 2006.
- Lauer, A.  
Untersuchung von Größenverteilung und Zusammensetzung des troposphärischen Aerosols mit einem globalen Zirkulationsmodell. Dissertation, Universität München. DLR-FB 2005-17, 2005.
- Nau, R.  
Das atmosphärische Aerosol-Vorläufergas SO<sub>2</sub>: Messungen mit einem flugzeuggetragenen Massenspektrometer. Diplomarbeit, Universität Heidelberg, 2004.
- Nau, R.  
Weiterentwicklung eines flugzeuggetragenen CIMS-Instruments: Spurengasmessungen in der Atmosphäre und in einem Blitzlabor. Dissertation, Universität Heidelberg, 2007.
- Schneider-Kühnle, Y.  
Experimentelle Untersuchung rußender Hochdruckflammen mit laserdiagnostischen Messmethoden. DLR Forschungsbericht, FB 2005-06, 2005.
- Schuck, T.  
Flugzeugmessungen troposphärischen Schwefeldioxids und Schwefelsäuremessungen im Abgas von Dieselmotoren. Dissertation, Universität Heidelberg, 2006.
- Spichtinger, P.  
Eisübersättigte Regionen. Dissertation, Universität München. DLR-FB 2004-21, 2004.
- Stenke, A.  
Stratosphärischer Wasserdampf in einem gekoppelten Klima-Chemie-Modell: Simulation, Trends und Bedeutung für die Ozonchemie. Dissertation, Universität München. DLR-FB 2006-04, 2006.